

2015

Live load distribution factors for multi-span girder bridges with plank decking subjected to farm vehicles

Chandra Teja Kilaru
Iowa State University

Follow this and additional works at: <https://lib.dr.iastate.edu/etd>

 Part of the [Civil Engineering Commons](#)

Recommended Citation

Kilaru, Chandra Teja, "Live load distribution factors for multi-span girder bridges with plank decking subjected to farm vehicles" (2015). *Graduate Theses and Dissertations*. 14399.
<https://lib.dr.iastate.edu/etd/14399>

This Thesis is brought to you for free and open access by the Iowa State University Capstones, Theses and Dissertations at Iowa State University Digital Repository. It has been accepted for inclusion in Graduate Theses and Dissertations by an authorized administrator of Iowa State University Digital Repository. For more information, please contact digirep@iastate.edu.

Live load distribution factors for multi-span girder bridges with plank decking subjected to farm vehicles

by

Chandra Teja Kilaru

A thesis submitted to the graduate faculty
in partial fulfillment of the requirements for the degree of

MASTER OF SCIENCE

Major: Civil Engineering (Structural Engineering)

Program of Study Committee:

Terry Wipf, Major Professor

Junwon Seo

Simon Laflamme

Zachary Lorren

Iowa State University

Ames, Iowa

2015

Copyright © Chandra Teja Kilaru, 2015. All rights reserved.

TABLE OF CONTENTS

LIST OF FIGURES	iv
LIST OF TABLES	v
ACKNOWLEDGEMENTS	vi
ABSTRACT	vii
CHAPTER 1. GENERAL INTRODUCTION	1
Problem Statement	1
Objective and Scope	2
Thesis Organization	3
CHAPTER 2. LATERAL LIVE LOAD DISTRIBUTION FOR MULTI-SPAN TIMBER GIRDER BRIDGES SUBJECTED TO FARM VEHICLES	4
Abstract	4
Introduction	5
Selected Bridges	8
Approaches	12
<i>AASHTO Specifications</i>	12
<i>Field Tests</i>	13
<i>FEA Simulations</i>	17
<i>Statistical Analysis</i>	21
Results and Discussion	23
Summary and Conclusion	26
Acknowledgements	28

CHAPTER 3. FARM VEHICLE INDUCED LATERAL LIVE-LOAD DISTRIBUTION FOR STEEL GIRDER BRIDGES WITH PLANK DECKING	29
Abstract	29
Introduction.....	30
Selected Bridges.....	33
Approaches	36
<i>AASHTO Specifications</i>	36
<i>Field Tests</i>	37
<i>FEA Simulations</i>	42
Results and Discussion	47
Summary and Conclusion.....	53
Acknowledgements.....	55
REFERENCES	56

LIST OF FIGURES

Figure 1: Representative photograph and cross-sectional view of bridge A	9
Figure 2: Representative photograph and cross-sectional view of bridge B	10
Figure 3: Representative photograph and cross-sectional view of bridge C	11
Figure 4: Farm vehicle configurations used for field testing.....	14
Figure 5: Strain data for bridge A.....	16
Figure 6: Strain data for bridge B	16
Figure 7: Strain data for bridge C	16
Figure 8: Finite element model of bridge B loaded with semi-truck.....	18
Figure 9: Cumulative Distribution Function (CDF) plots for Bridge A, B and C.....	22
Figure 11: Graphical representation of results for bridge B	24
Figure 12: Graphical representation of results for bridge C	25
Figure 13: Overview of the location of the bridge B4.....	34
Figure 14: Photographs of bridge B4 (a) Elevation view (b) Steel girders	35
Figure 15: Cross-section of bridge B4.....	35
Figure 16: Photographs of vehicles used for field testing	39
Figure 17: Location of vehicle during field testing	40
Figure 18: Sample strain plot of all test vehicles.....	41
Figure 19: Strain plot of all girders for bridge B4	42
Figure 20: Finite element model of bridge B4 loaded with terragator	45
Figure 20:(a-k) LLDFs for Field Tested Steel-Timber bridges.....	51

LIST OF TABLES

Table 1: Selected timber bridges' characteristics	8
Table 2: Initial and calibrated values of geometric parameters for bridges A, B and C.....	20
Table 3: Statistical Results for bridges A, B and C	20
Table 4: Percent Difference between Statistical LLDFs and AASHTO Specifications for bridges A, B and C.....	24
Table 2: Selected steel-timber bridges' characteristics	33
Table 6: Vehicle configurations used for field testing.....	40
Table 7: Initial and calibrated values for bridge structural components.....	46
Table 8: Initial and calibrated values for bridge structural components.....	52
Table 9: Percent difference between AASHTO Specified LLDFs and Statistical Limits for Field Tested Steel-Timber Bridges	53
Table A1: Farm Vehicle Inventory	53

ACKNOWLEDGEMENTS

I wish to express my sincere thanks to my major professors, Dr. Terry Wipf and Dr. Junwon Seo. Specially, I am deeply gratified that Dr. Junwon Seo as my advisor and mentor provided me with critical comments and support at all stages of this research. Through my thesis, I would like to give my special thanks to him. I gratefully acknowledge Dr. Brent Phares for giving me the opportunity to work on this research and required financial assistance over the last two years. He supported me and provided the much needed encouragement. I would also like to acknowledge Dr. Simon Laflamme and Dr. Zachary Lorren for their co-operation and involvement in this research and also, for being part of my advisory committee.

I am thankful to my family and Samhitha for their moral support, encouragement, and motivation throughout my life. I gratefully acknowledge my dear friend Venkata for his companionship and moral support. I would like to thank Rachana for helping me in the automation process for my analytical study. I would also like to thank all my friends— Venu, Loukya, Vigna, Satish, Venky, Alekya, Anirudh, Rohini, Sudheer, and Pranava for their companionship and being with me in my tough times.

Finally, I am thankful to Iowa State University for providing me this great opportunity.

ABSTRACT

The American Association of State Highway and Transportation Officials (AASHTO) specifications provide simplified formulae to determine Live Load Distribution Factors (LLDFs) for highway bridges. The formulae for the AASHTO code-specified LLDFs have been developed, considering the effect of typical highway trucks. In addition to highway bridges, there are a large number of bridges located on secondary roadways where farm vehicles having varying configurations and weights frequently travel. Unfortunately, LLDFs for the bridges loaded with farm vehicles are not well known. In this study, hence, two bridge types, including steel girder bridges with plank decking and timber girder bridges with plank decking, were selected to determine LLDFs of the bridges under the effects of farm vehicles. The procedure adopted include the AASHTO code-specified formulae, field testing, finite element modeling, and analytical simulations of all the bridges. Field testing of each bridge was conducted with four different farm vehicles and a five-axle highway truck used as a benchmark for exploring highway truck-induced LLDFs. Commercially available Finite Element Analysis (FEA) software was utilized to generate analytical models of all the bridges, and the models were calibrated with field data. To consider the effects of vastly different farm vehicles, information on 121 existing farm vehicles were collected and used as input loads in the models to compute analytical LLDFs for the bridges. The analytical LLDFs resulting from 121 farm vehicles were used to establish statistical limits representing deterministic values for LLDFs for each bridge. The field, analytical, and statistical LLDFs were compared to those obtained from the AASHTO specifications. Results showed that the AASHTO LLDFs were, in some cases, inadequate for the timber girder bridges, while those were, in most cases, adequate for the steel girder bridges.

CHAPTER 1. GENERAL INTRODUCTION

In the United States, highway bridges are designed based on the American Association of State Highway and Transportation Officials (AASHTO) Specifications. These specifications were developed based on extensive research done by many researchers and revised, reflecting new research and developments. However, the AASHTO specifications for Lateral Live-Load Distribution Factors (LLDFs) for timber deck bridges remain unchanged for many years. The timber deck bridges include timber girder bridges with plank decking and steel girder bridges with plank decking. According to the statistics of National Bridge Inventory (NBI), timber deck bridges constitute approximately ten percent of all bridge types [1]. In addition to the NBI, the US Department of Agriculture (USDA) Forest Service owns 7,500 timber bridges [2]. More timber bridges are built nationwide by Departments of Transportation and USDA each year. Similar to the percentage of national timber bridges, approximately 11 percent of all bridges located in Iowa consist of timber deck bridges [1]. The most benefits from the continuous use of timber bridges are their light-weight, sufficient strength, energy-absorbing properties, and environment-friendly construction materials, respectively. Further, timber is seldom critically damaged by continuous freezing or thawing [1]; thus, timber deck bridges with the benefits can be efficiently constructed in any environmental conditions.

Problem Statement

The majority of timber bridges are often located on secondary roadways where heavy farm vehicles are used for agricultural purposes. Heavy tractors combined with farm implements have a wider range of geometries and weights; thus, their variability can result in different LLDFs compared to conventional highway trucks. LLDFs can generally be defined as the ratio of the maximum live-load effect in a single component to the maximum live-load effect in a system when using beam-line model techniques [3]. The current AASHTO specifications provide formulas (s-over rule) specific to LLDFs

developed for timber bridges under the effects of conventional highway trucks [4]; [5]. The s-over formulas consider only girder spacing in evaluating LLDFs and neglects the effect of other parameters associated with bridge geometry and vehicle configurations. The s-over formulas for timber bridges proved either to be too permissive or too conservative in some cases [6]; [7]. Further, sophisticated parametric formulas as a function of multiple bridge geometric factors were developed for other bridge types such as steel-concrete composite girder bridges by the extensive research work of National Cooperative Highway Research Program (NCHRP) 12-26 report (Zokaie et al. 1993). The LLDFs equations presented in the AASHTO LRFD Design Specifications 2005 [5] have been adopted from the work of NCHRP report [3]. The database consisted of 365 slab-on-girder bridges but timber deck bridges were not included in the database. Also, the NCHRP report [3] neglected the effect of farm vehicle configurations. Therefore, it is necessary to accurately predict LLDFs for timber deck bridges considering the effects of farm vehicle loadings. Specifically, the focus of this study is on LLDFs determination of timber girder bridges with plank decking and steel girder bridges with plank decking.

Objective and Scope

The overall objective of this study presented herein is to evaluate the live load distribution provisions provided in the AASHTO Specifications [4]; [5] in relation to timber deck bridges under farm vehicle loadings. The objectives listed above were accomplished by completing the following tasks:

1. Review LLDFs provisions in the AASHTO LRFD Bridge Design specifications for timber deck bridges.
2. Select in-service bridges (including timber girder bridges with plank decking and steel girder bridges with plank decking) for field tests with actual farm vehicles and a conventional highway truck
3. Determine LLDFs from AASHTO Specifications and field LLDFs from field testing results respectively

4. Develop analytical models for the selected bridges using commercially available Finite Element Analysis (FEA) software
5. Calibrate the models using field data
6. Determine analytical LLDFs for the bridges under different farm vehicles (including test vehicles).
7. Determine statistical limits based upon a basic probability theory. .
8. Compare analytical and statistical LLDFs against those obtained from the AASHTO specifications and field tests.

Thesis Organization

This thesis is composed of two papers: Chapter 2: LLDFs for timber girder bridges and Chapter 3: LLDFs for steel girder bridges. Chapter 2 is entitled “Lateral Live Load Distribution for Multi-Span Timber Girder Bridges Subjected to Farm Vehicles.” This presents the load distribution in timber girder bridges with timber decking subjected to farm vehicles. This was accomplished by codified processes, field testing, and finite element analysis for three selected timber-timber bridges in Iowa. Detailed procedure of different approaches adopted in evaluating LLDFs was presented. The analytical results were then compared with the results from the field testing and AASHTO specifications. Chapter 3 is entitled “Farm Vehicle-Induced Lateral Live-Load Distribution for Steel Girder Bridges with Timber Deck”. This is intended to determine LLDFs of steel girder bridges with timber deck subjected to farm vehicles. Eleven steel-timber bridges were selected in Iowa. The same procedure of field testing and finite element analysis in Chapter 2 was discussed for one of the representative bridges. The analytical results were then compared with those resulting from the field testing and AASHTO specifications.

CHAPTER 2. LATERAL LIVE LOAD DISTRIBUTION FOR MULTI-SPAN TIMBER GIRDER BRIDGES SUBJECTED TO FARM VEHICLES

Modified from a paper to be submitted to Journal of Bridge Engineering

Abstract

Farm vehicles with varying configurations and weights are frequently driven over timber bridges on secondary roadways in the United States. Lateral Live-Load Distribution Factors (LLDFs) for the bridges loaded with farm vehicles are not well known. Further, the effects in association with farm vehicles have not been considered in current American Association of State Highway and Transportation Officials (AASHTO) Specifications that solely provide simplified formulas to determine LLDFs of timber girders. To more explicitly estimate the timber girder LLDFs, three multi-span timber girder bridges in Iowa were selected and each of the girder LLDFs were determined based upon various methods, including codified processing, field testing, simulating, and statistical analyzing. For field LLDFs, the bridges were tested with four different farm vehicles and a five-axle highway truck used as a benchmark for exploring highway vehicle LLDFs. As part of analytical LLDF investigation, analytical models of the bridges were generated and calibrated with field data using commercially available Finite Element Analysis (FEA) software. To consider the effects of vastly different farm vehicles on analytical bridge LLDFs, information on 121 existing farm vehicles were collected and used as input loads in the models to compute analytical LLDFs for the bridges. The LLDFs resulting from 121 farm vehicles were used to establish statistical LLDF limits representing deterministic values for each bridge. All resulting LLDFs were compared to those determined from the AASHTO Specifications, showing that the AASHTO specified LLDFs were, in specific cases, inadequate for the bridges.

Introduction

Heavy tractors combined with farm implements are commonly driven over timber bridges on secondary roads in the United States. Farm vehicles' characteristics, which are different from traditional highway trucks, can cause dissimilar Live-Load Distribution Factors (LLDFs). Therefore, determining accurate LLDFs served as the basis for reasonably designing and rating timber girder bridges under the effects of farm vehicles is needed. Generally, LLDFs for any girder bridges can be defined as the ratio of the maximum live-load effect in a system to the maximum live-load effect in a single component when using beam-line model techniques [3]. The LLDFs for timber bridges can be simply determined based upon a s-over rule provided by the American Association of State Highway and Transportation Officials (AASHTO) Specifications [4]; [5]. The AASHTO specified LLDFs have widely been in use for designing and rating different types of timber girders since 1930s [8]. However, the s-over rule in both the AASHTO Standard and LRFD Specifications has only considered girder spacing to calculate the LLDFs [4]; [5]. The AASHTO Specifications neglects the effects of other parameters associated with bridge and vehicle configurations. Although more sophisticated parametric equations developed by the extensive research work of National Cooperative Highway Research Program (NCHRP) 12-26 report have been adopted and available in the AASHTO LRFD Specifications, the focus was on typical steel girder bridges, not timber girder bridges [9].

In addition to the NCHRP 12-26 report, most studies investigating bridge load distribution characteristics have focused on field tests and Finite Element Analysis (FEA) based simulations for steel girder bridges loaded with normal highway trucks. Most of these studies have neglected to explore the effects of farm vehicle characteristic parameters on LLDFs ([10]; [9]; [11]; [12]; [13]; [14]). In the past studies, the LLDFs resulting from highway trucks were compared to those from the AASHTO Specifications, indicating that the AASHTO LLDFs are either too permissive or too conservative in most cases. For example, Tarhini et al. (1992) developed flexural load distribution formulas for highway steel I-girder bridges using FEA [11]. It was concluded that the calculated

LLDFs were lower than those from the AASHTO Specifications. Bishara et al. (1993) generated FEA models to determine analytical LLDFs for highway steel I-girder bridges in Ohio [12]. It was found that the AASHTO specified LLDFs are very conservative as well. Kim and Nowak (1997) attempted to determine field LLDFs for highway steel I-girder bridges located in Michigan, showing these LLDFs were lower than the AASHTO Specifications-compliant LLDFs [13]. Elisa et al. (2004) carried out FEA on 60 selected steel girder bridges and prestressed concrete girder bridges and developed new simplified equation for LLDFs [15]. It was observed that the new equation produced more conservative LLDFs for these bridge types as compared to the AASHTO Specifications. Eom and Nowak (2006) performed field tests and FEA on highway five two-lane steel I-girder bridges [15]. It was found that AASHTO specified LLDFs were conservative for the bridge LLDF determination. Meanwhile, a recent study (Seo et al. 2013) sheds some light on the origins of the agricultural load LLDFs of steel I-girder bridges with concrete decking [16]. Specifically, the LLDFs of five simply supported steel girder bridges under passage of farm vehicles were determined in an experimental and analytical manner. The resulting LLDFs were compared to the AASHTO specified LLDFs, showing that the most LLDFs were not greater than the AASHTO values. However, some LLDFs were greater than the AASHTO values. It was concluded that agricultural loads had an influence on the LLDFs for all the five bridges.

Compared to extensive studies on the LLDFs of steel girder bridges, a relatively small number of studies have attempted to determine LLDFs for different timber bridge types using field tests and/or FEA simulations [17]; [6]. Ritter et al. (1998) tried studied the live load distribution in single span longitudinal stringer bridges with transverse deck panels [17]. Fanous et al. (2011) attempted to investigate the effect of bridge configuration parameters on the LLDFs for glue laminated timber girder bridges subjected to highway trucks [6]. They also developed new LLDF equations for the bridge group based upon the results from their FEA simulations. It was revealed that AASHTO LRFD Specifications for LLDFs overestimated the live load distribution of glued-laminated timber bridges. Again, these studies have solely focused on the LLDF investigation for highway-type vehicles, neglecting the effects of variability in farm

vehicles. Since distinctive characteristics on farm vehicles can lead to more diverse LLDFs compared to those resulting from highway trucks (Seo et al. 2013), the LLDFs for timber bridges under agricultural loads need to be investigated to make some recommendations for timber bridge LLDFs in the AASHTO Specifications [16].

This study is aimed to explicitly explore LLDFs of timber bridges under the passage of varying farm vehicles. In an attempt to accomplish the aim of the study, this paper is structured into five sections. The opening section presents detailed information of three multi-span timber girder bridges selected for this study. The next section describes various approaches, which include the codified process, field tests, simulations, and statistical analyses, to determine LLDFs for all three bridges. Then, resulting LLDFs obtained from each approach are provided and compared each other in the following section, investigating their similarities and dissimilarities between the LLDFs for all three bridges. The final section highlights some insights from this study and provides some recommendations for future work.

Selected Bridges

Three continuous multi-span timber bridges located on a rural roadway in Audubon County in Iowa were selected for this study. Each of the bridges has multiple timber girders with plank decking. The bridge characteristics are summarized in Table 1. Representative photographs and cross-sections for each bridge are shown in Figures 1, 2, and 3, respectively. Bridge A classified as two traffic lanes has two equal spans of 4.6m and zero skew supports. Bridge B carrying two-way traffic is a three span timber girder bridge. It has a total span length of 18.9m from center to center of abutments. The first, second, and third span lengths are 5.8m, 7.3m, and 5.8m, respectively. Bridge C carrying two-way traffic has a total span length of 18.9m. This bridge has two unequal spans of 9.8m and 9.1m. For bridges A and C, the 7.6cm thick timber deck and for bridge B, the 15.3cm thick timber deck was in satisfactory condition according to the Iowa DOT inspection data.

Table 1: Selected timber bridges' characteristics

Bridge	NBI No.	Number of Spans	Span Length (m)	Average Girder Spacing (m)	Number of girders	Width (m)	Deck Thickness (cm)	Skew (degree)
A	B68790	2	9.1	0.3	17	5.5	7.6	0
B	B68800	3	18.9	0.31	27	6.1	15.2	25
C	B68930	2	18.9	0.31	18	5.4	7.6	30

Note: NBI stands for National Bridge Inventory

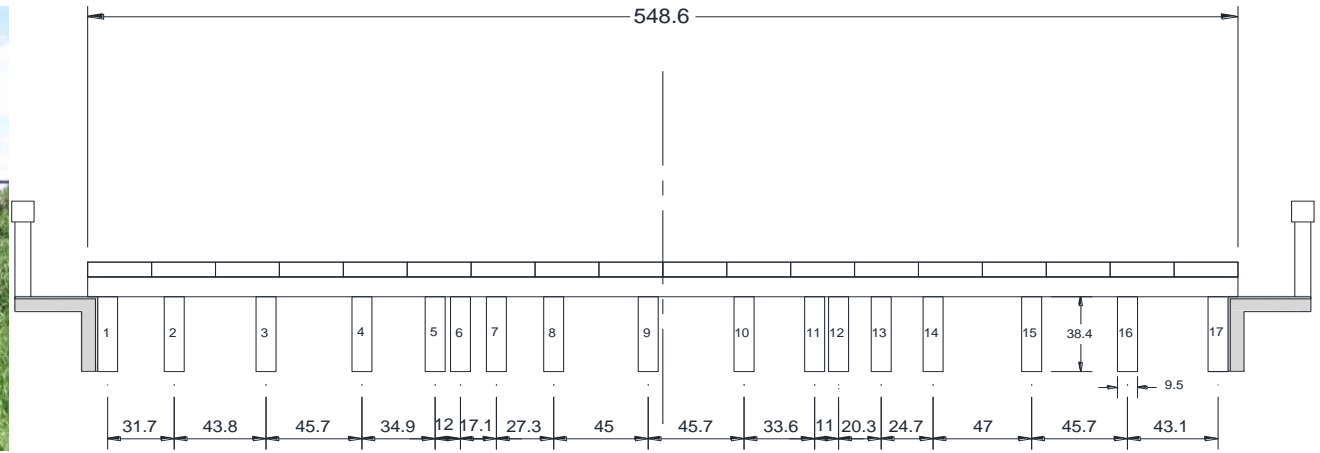


Figure 1: Representative photograph and cross-sectional view of bridge A (units: centimeters)

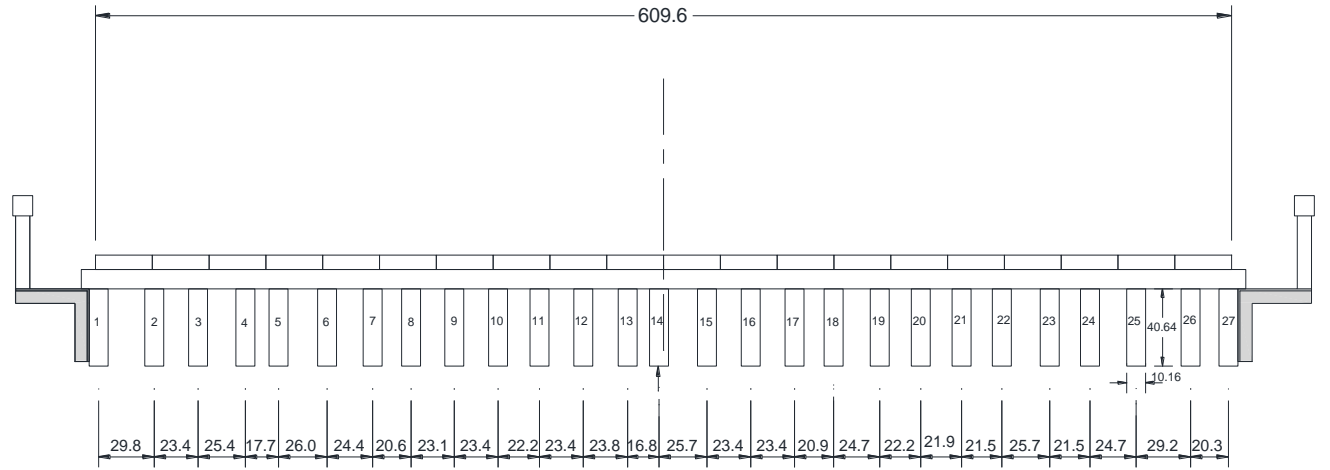


Figure 2: Representative photograph and cross-sectional view of bridge B (units: centimeters)

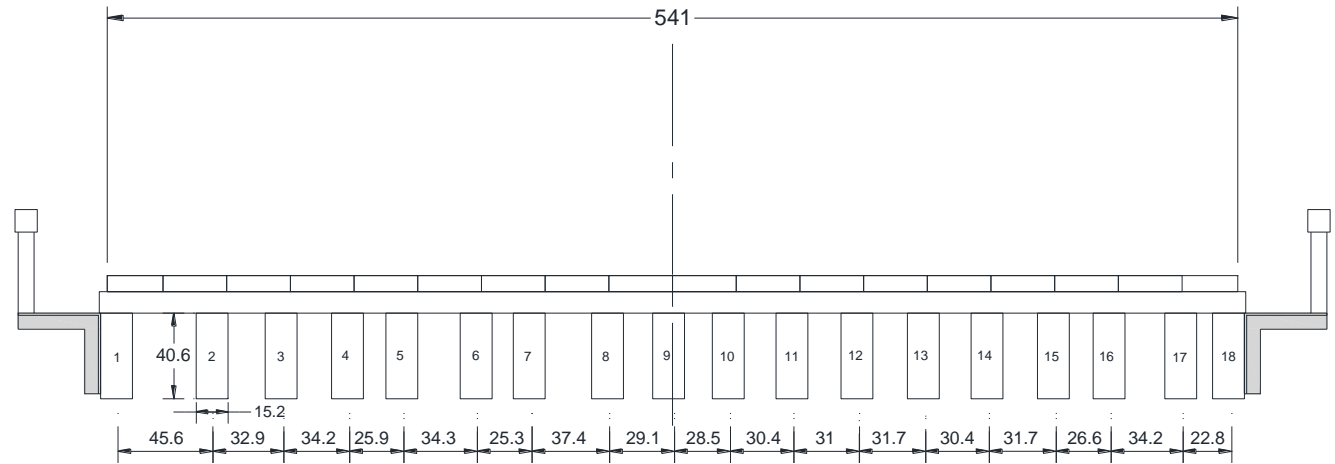


Figure 3: Representative photograph and cross-sectional view of bridge C (units: centimeters)

Approaches

LLDFs for the select bridges are determined based upon the AASHTO Specifications, field tests, FEA simulations, and statistical analysis. Details for each approach are presented in the following sections.

AASHTO Specifications

The AASHTO Standard and LRFD Specifications, which serve as a basis to evaluate the rationality of experimental and analytical LLDFs, can be used to determine LLDFs for typical timber bridges [4]; [5]. Both specifications provide LLDF equations developed based upon the s-over rule, which is a function of girder spacing and bridge type factor. The concept, assumptions and drawbacks when using the s-over equations were presented by Bakht and Moses (1987) [10]. In the AASHTO Standard Specification of interior girders for timber bridges with plank decking, the LLDF for a single traffic lane is

$$DF = \frac{s}{13.1} \quad (1)$$

and for multiple traffic lanes

$$DF = \frac{s}{12.3} \quad (2)$$

In the AASHTO LRFD Specification of interior timber girders with plank decking, the LLDFs for a single traffic lane is

$$DF = \frac{s}{22.0} \quad (3)$$

and for multiple traffic lanes

$$DF = \frac{s}{19.6} \quad (4)$$

where 's' is the average spacing between the adjacent girders (m).

The AASHTO LLDFs for interior girders of all three bridges should be multiplied by 0.5 to make it applicable to a full truck because it has been derived for wheel loads [6]. Note that the *lever rule* recommended by the AASHTO Specifications was used to determine the LLDFs of exterior girders for the bridges. The *lever rule* is a method of computing the LLDF by summing moments about the first interior girder, assuming a notional hinge to obtain the reaction at the exterior girder [18]. More details on the *lever rule* can be found in the AASHTO LRFD Specifications (2010) [5].

Field Tests

Field testing is a key process to obtain actual data necessary for determining field LLDFs for individual girders of each bridge. Bridge Diagnostics Inc. was used as field data acquisition system for strain gage measurements during field tests of all the bridges [19]. A network of multiple strain gages attached to the bottom flanges of all girders was used to measure strain quantities via the BDI for each bridge under passages of testing vehicles. The testing vehicles consisted of four farm vehicles and one highway truck. The farm vehicles included a terragator, a grain cart, a honey wagon with one tank, and a honey wagon with two tanks, while the highway truck contained a five-axle semi-truck. As shown in Figure 4, the configurations for the farm vehicles selected for the testing were different from that of the highway truck.

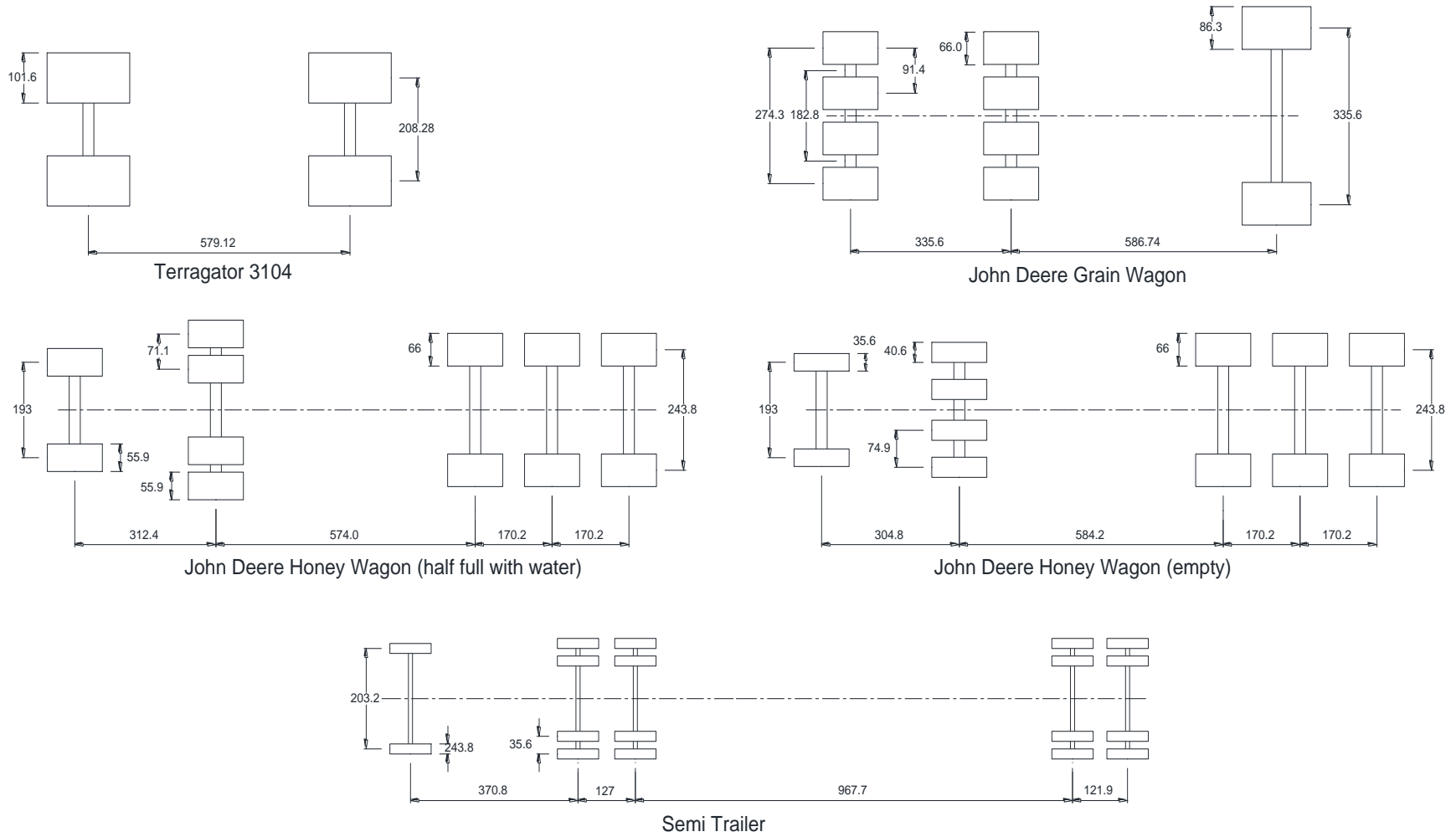


Figure 4: Farm vehicle configurations used for field testing

During the testing process, one test vehicle at a time was driven across each bridge at a crawl speed at the centerline of the bridge and field strains to each vehicle passage were measured for each bridge. Figures 5, 6 and 7 show the plots of strain data for one of the interior girder for all the three bridges A, B and C under each passage of five test vehicles, respectively. In these figures, the maximum magnitudes of strain data occur for central girders at the center of the bridge as each of the test vehicles travels through the centerline. Although the semi-truck normally results in higher strains compared to other farm vehicles, the terragator occasionally yields somewhat greater strains than the truck. This tendency can be seen in Figure 5 and 6. These strains were employed to determine field LLDFs for each girder based upon the following equation:

$$DF^f = \frac{\epsilon^m_{\max i, t}}{\sum_{i=1}^n \epsilon^m_{\max i, t}} = \frac{M^m_{\max i, t}}{\sum_{i=1}^n M^m_{\max i, t}} \quad (5)$$

where DF^f is the field LLDF and ϵ^m and M^m are the measured maximum strains and moments for individual girders over time.

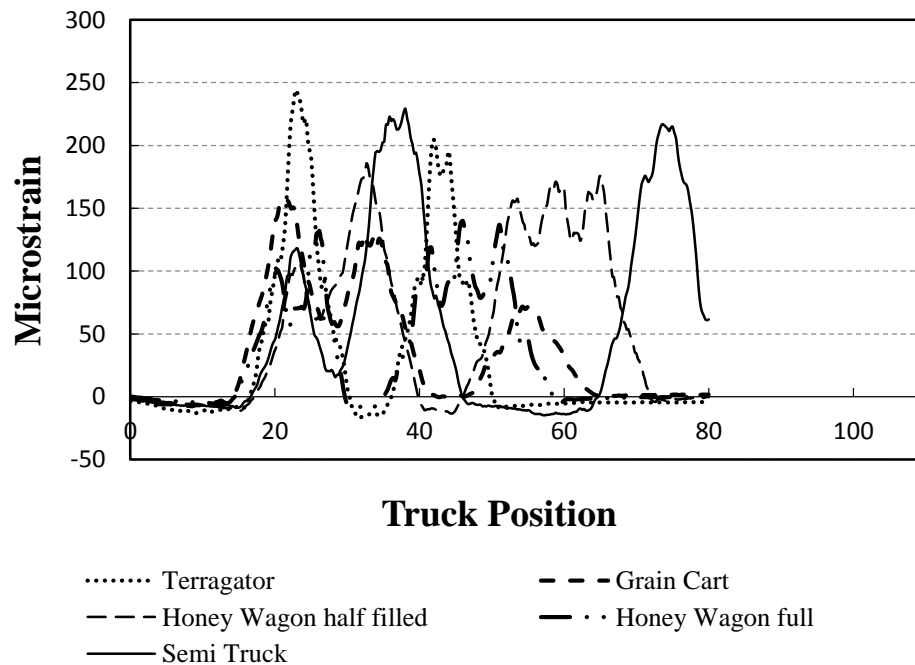


Figure 5: Strain data for bridge A

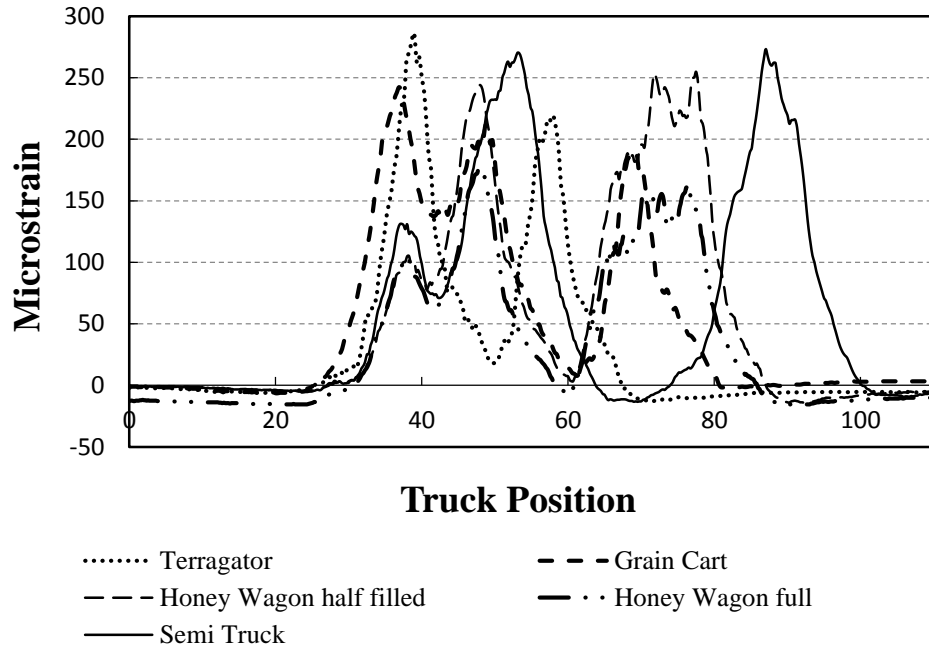


Figure 6: Strain data for bridge B

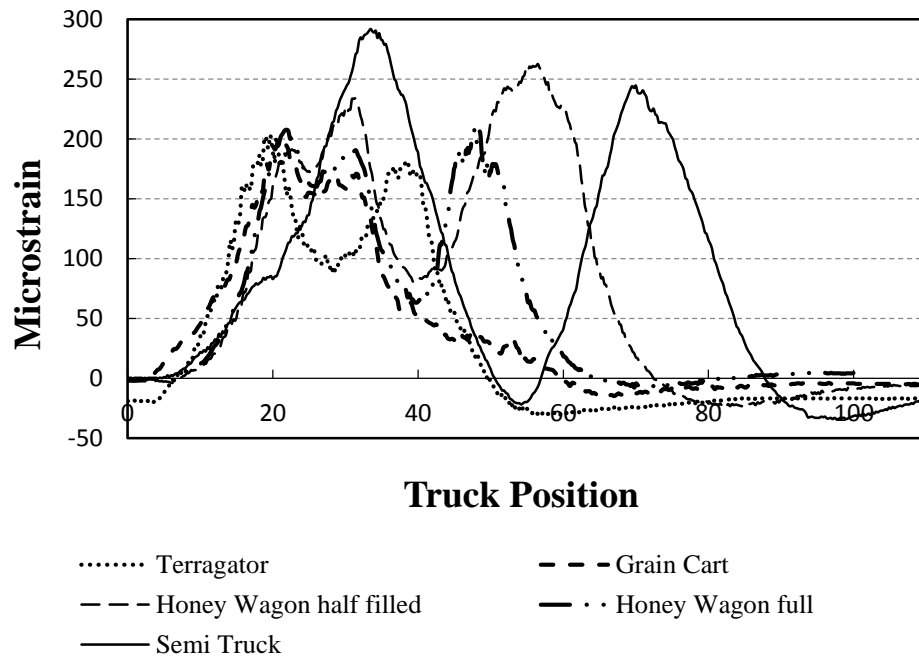


Figure 7: Strain data for bridge C

FEA Simulations

The field testing helps bridge engineers determine actual LLDFs for the bridges, but it is required that the testing with a great effort be carried out at bridge sites using expensive field equipment. Besides, the field testing is not an efficient approach when the further investigation of LLDF characteristics for bridges loaded with a large number of different agricultural vehicles is needed. As such, FEA simulations have been considered efficient for reasonably determining LLDFs for typical steel or timber girder bridges ([20]; [11]; [12]; [21]; [6]). Hence, analytical LLDFs for the bridges were determined based upon the FEA simulations and the effects of 121 different farm vehicles on LLDFs were evaluated. A detailed description of the FEA simulation-based approach is presented in the following subsections.

Model Generation

Each of the bridges was initially modeled with appropriate geometric and material properties using BDI finite element software [19]. The geometric information, such as girder spacing, was obtained from the bridge plans and/or field inspections. The modulus of elasticity of 11,032 MPa was assigned for all timber components in the models based upon the AASHTO LRFD Specification [5]. Each FEA model consists of beam elements for timber girders, shell elements for a timber deck, and rotational springs necessary for simulating actual behavior of supports such as abutments and bearings at piers. Figure 8 shows a representative model of bridge B loaded with a semi five-axle truck

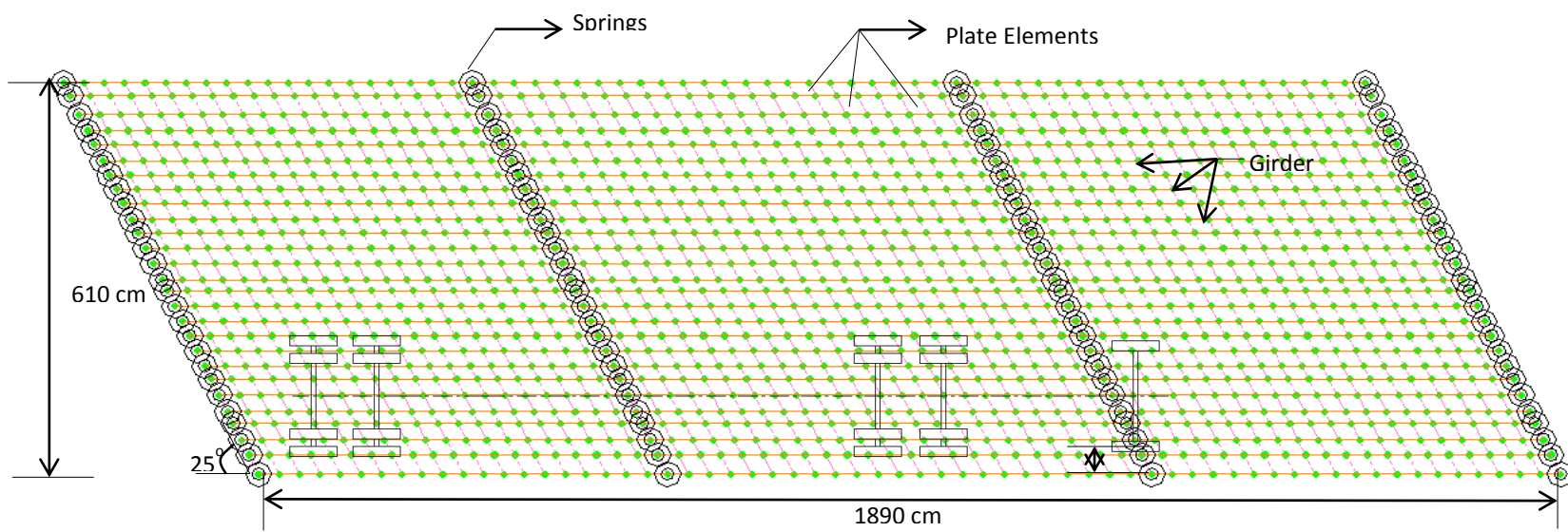


Figure 8: Finite element model of bridge B loaded with semi-truck

Model Calibration

After the model generation, each model was calibrated with field data. The model calibration means the iterative process to obtain the highest correlation and the lowest errors between the analytical and field responses. This was accomplished by altering sectional and/or material properties for each model within reasonable limits that were established by previous work [16]; thus, this made the model as accurate as possible and this ended up reasonably predicting actual behavior of each bridge. Calibration parameters that were same for all the three bridges included modulus of elasticity and moment of inertia for timber girders and decks and rotational stiffness at the supports. Their values were adjusted within predetermine limits during a calibration process of each model. For each of the iteration processes, a graphical user interface tool in the BDI software was utilized to graphically and statistically make a comparison between field and analytical results. The same procedure was repeated with each of the testing vehicle and model parameters were modified within the established limits. Table 2 shows initial values and calibrated values along with corresponding errors for all three bridges. For the model calibration of Bridge A, four different cross-sections were used for girders G2 and G16, G6 and G7, G11 and single cross-section for remaining girders respectively. A single cross section was considered for deck elements and support connections. For bridge B and C, single cross section was considered for all the model parameters.

The model accuracy is measured using the parameters percent error (δ_p) and correlation coefficient ($\rho_{f,a}$) [16]. Percent error (δ_p) and correlation coefficient ($\rho_{f,a}$) measure the strain variation and linear relationship of analytical results and field testing data. Lower the percent error and higher the correlation coefficient indicates that model is able to replicate the behavior of the bridge in situ. Table 3 summarizes the minimized errors and correlation coefficients for all the three selected bridges. The calibration process resulted in models with accuracy 82.8%, 78.1% and 76.2% for bridges A, B and C respectively. The reduction in model accuracy for all the three bridges was due to uncertainty in timber materials deteriorating over time and complicated inelastic structural behavior caused by non-uniform girder spacing resulting in extremely high strain quantities for some girders.

Table 2: Initial and calibrated values of geometric parameters for bridges A, B and C

Calibration Parameters	Bridge Components	Bridge A		Bridge B		Bridge C	
		Initial	Final	Initial	Final	Initial	Final
Moment of Inertia (cm ⁴)	Exterior Girder	5.7E+04	7.1E+04	5.7E+04	4.5E+04	8.5E+04	7.7E+04
	Interior Girder	5.7E+04	7.1E+04	5.7E+04	4.5E+04	8.5E+04	7.7E+04
Modulus of Elasticity (Mpa)	Deck	1.1E+04	8.3E+03	1.1E+04	8.3E+03	1.1E+04	8.3E+03
Rotational Stiffness (kN-m/rad)	Support Connections	0.0E+00	4.1E+03	0.0E+00	7.8E+03	0.0E+00	1.8E+03

Table 3: Statistical Results for bridges A, B and C

Statistical Results	Bridge		
	A	B	C
δ_p	17.1%	21.9%	23.8%
$\rho_{f,a}$	0.92	0.88	0.86

121 Farm Vehicles

Once the model calibration was completed, each model was applied by each of 121 farm vehicles having different axle spacing, weights, and gage widths. This was accomplished to explore the effects of variability in the farm vehicle characteristics on LLDFs for all three bridges. Note that the 121 farm vehicles used for this study completely differ in their characteristics from one to another. The data was taken from different suppliers who sell farm vehicles for agricultural purposes nationwide. Detailed characteristics for the farm vehicles can be found elsewhere (Seo et al., 2013). Each vehicle travels across each of the models covering all the transverse locations. It is worthwhile to state that the transverse vehicle positions varied depending on the distance between the vehicle width and bridge width measured from curb to curb. As an example of the vehicle positions, the transverse location of five-axle truck positioned at one of the nearest curbs of the Bridge

B's model according to the AASHTO Specifications [5] can be seen in Figure 8. Strain response was recorded with the help of strain gages defined in the model at the same location as the field testing was done. This strain data was used to compute analytical LLDFs for each simulation for all the 121 farm vehicles using the Eq. (5). Followed by, extraction of maximum analytical LLDFs among all the simulations for each girder.

Statistical Analysis

As stated previously, the AASHTO Specifications provide LLDF equations to determine a single LLDF value for a group of interior girders and of exterior girders for timber bridges. To ease the comparison of all analytical LLDFs for individual girders with those from the AASHTO Specifications and to interpret the results efficiently, the LLDFs of all the girders of each bridge were grouped into interior and exterior girder LLDFs. Statistical analysis was completed on the computed analytical LLDFs for each girder group of all three bridges based upon a basic probabilistic theory, resulting in their discrete Cumulative Distribution Functions (CDFs). CDF plots show the variation trend of analytical DFs and help us to determine any statistical limit in interest. Statistical interior and exterior girder LLDF limits for the bridges were defined to be the 95% confidence thresholds, showing the probability that computed LLDFs are beyond the thresholds of 5%. Figure 12 include CDF plots for all the three bridges A, B and C showing the probability distribution of LLDFs. To determine each statistical limit, the limits for each bridge were estimated to be the realization values at a 95% probability obtained from the CDFs. Further information related to the statistical LLDF determination can be found in past work (Seo et al. 2013).

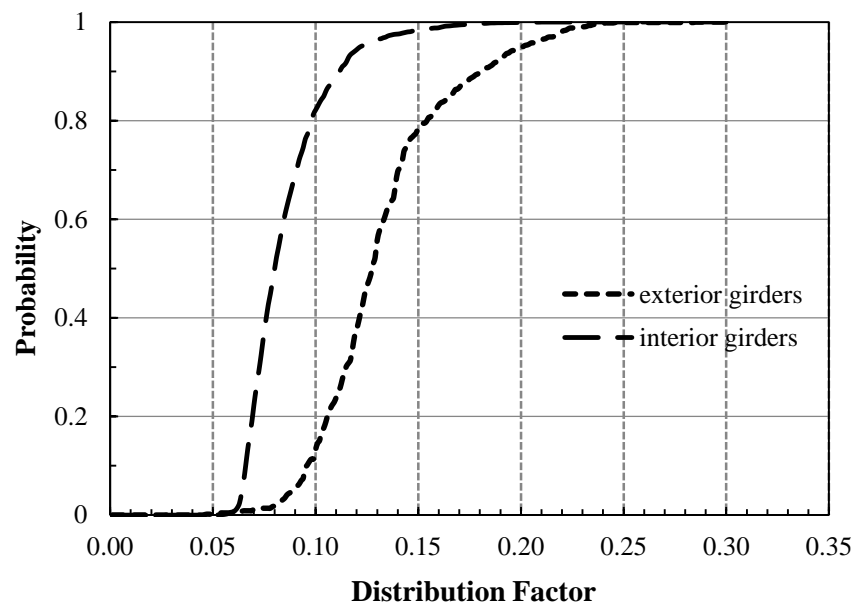
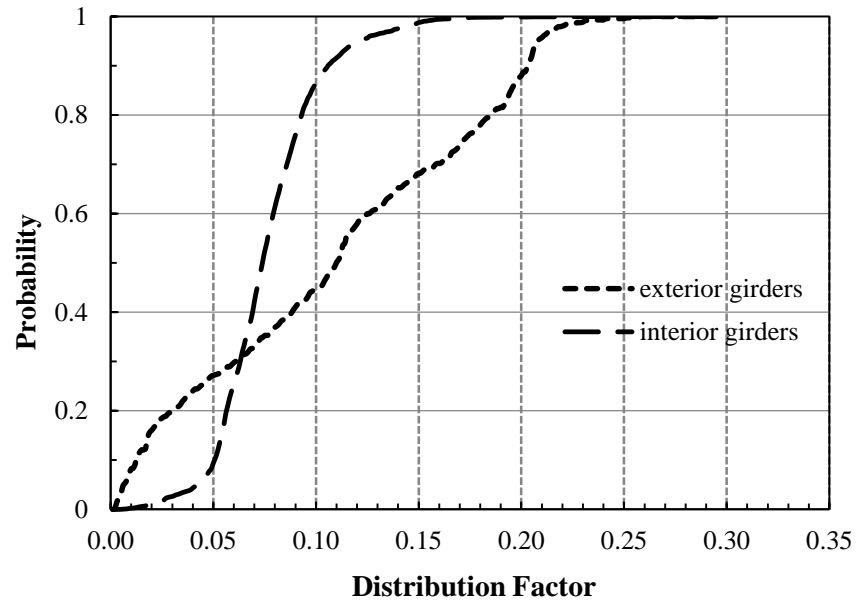
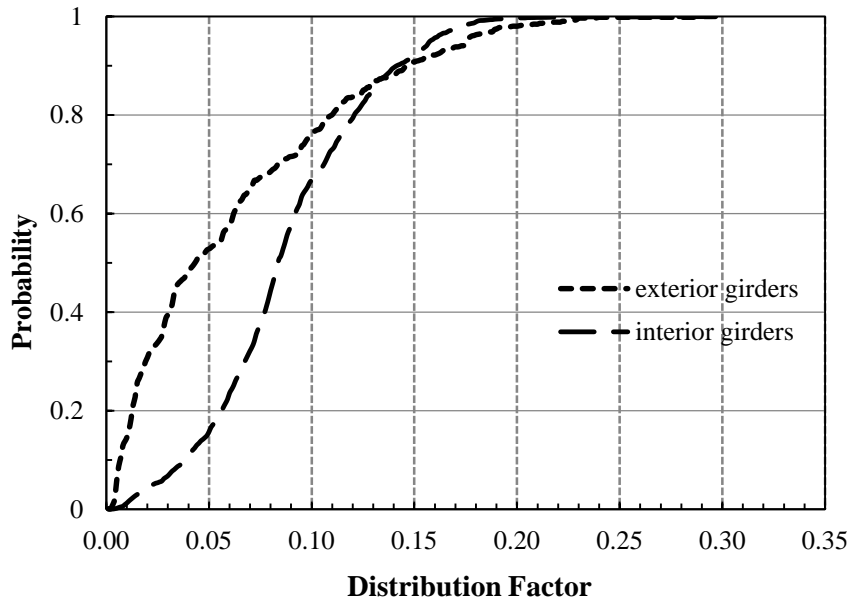


Figure 9: Cumulative Distribution Function (CDF) plots for Bridge A, B and C

Results and Discussion

The effect of farm vehicles on LLDFs were investigated via comparison of results obtained from field testing, analytical simulations, and AASHTO Specifications. All girder LLDFs for bridges A, B, and C are presented in the Figures 10, 11 and 12, respectively. Each figure includes envelopes of LLDFs obtained from field testing and analytical simulations for each girder; these values vary from girder to girder. Whereas, single values for each group of exterior and interior girders were determined from AASHTO Specifications and statistical analysis.

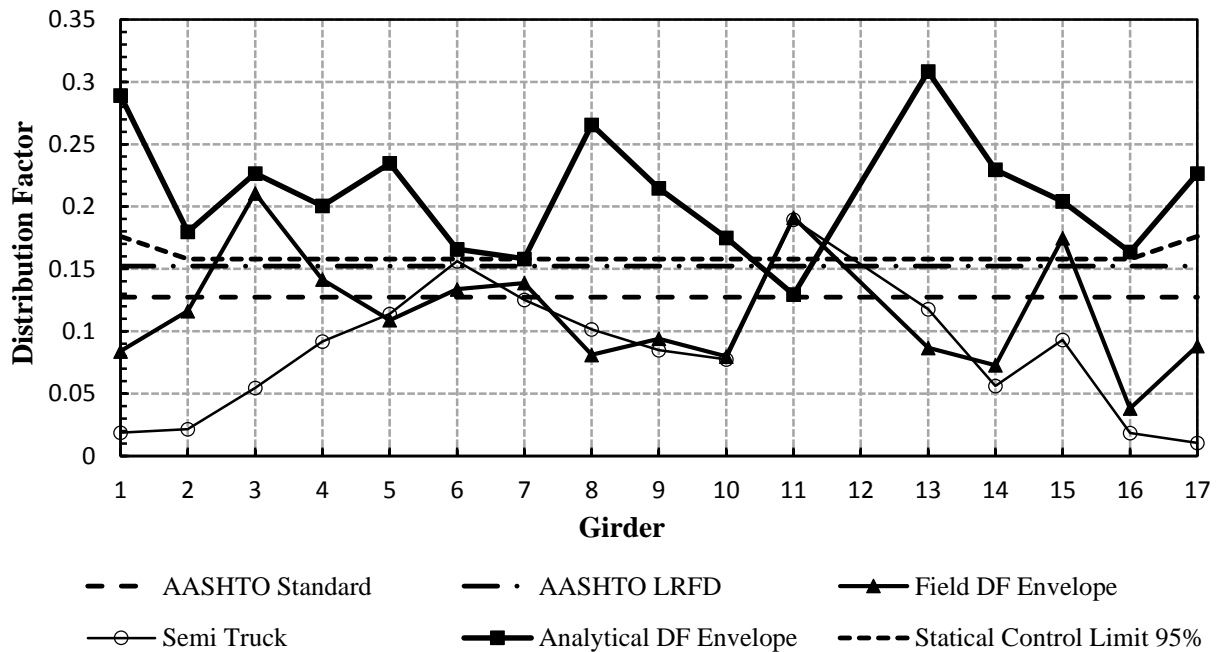


Figure 10: Graphical representation of results for bridge A

The LLDF envelope for bridge A is shown in Figure 10. It can be observed that the analytical LLDF envelope has values larger than AASHTO Specifications, except for G11. The maximum analytical LLDF of exterior girders is observed in G1 which has the LLDF of 0.29, while that of interior girders was found in G13 which has the LLDF of 0.31. These values are much higher when compared to the AASHTO LLDF limits. Figure

10 indicates that the field LLDF envelope has values larger than that for the semi truck for most of the girders. The 95% statistical limit for interior and exterior group of girders also has values larger than AASHTO Specifications. Table 4 summarizes the percent differences between the AASHTO values and statistical limits for bridges A, B and C. The statistical limit determined shows 27.6 and 10.2% greater values than AASHTO Standard [4] and AASHTO LRFD Specifications [5] for exterior girders; 19.3 and 3.7% greater values for interior girders.

Table 4: Percent Difference between Statistical LLDFs and AASHTO Specifications for bridges A, B and C

Bridge	Exterior LLDF		Interior LLDF	
	AASHTO Standard	AASHTO LRFD	AASHTO Standard	AASHTO LRFD
A	27.6%	10.2%	19.3%	3.7%
B	61.8%	61.8%	57.9%	57.9%
C	54.8%	46.0%	43.7%	32.8%

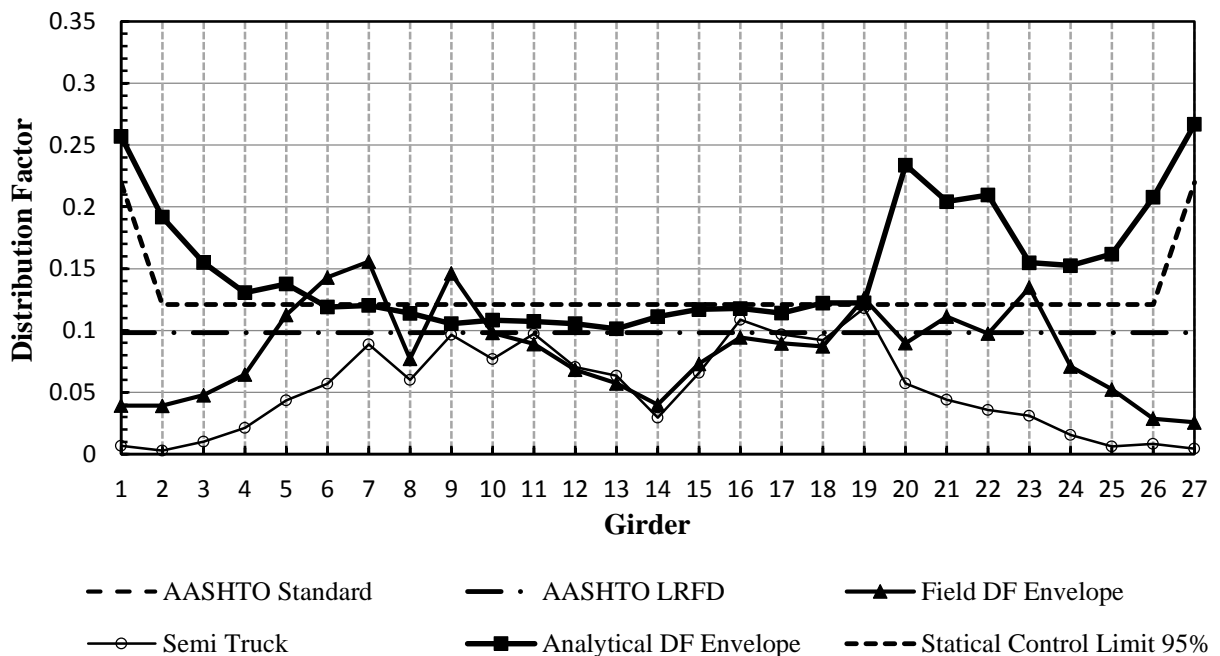


Figure 10: Graphical representation of results for bridge B

The LLDF envelope bridge B is shown in Figure 11. The bridge B supporting two way traffic (bridge width ≥ 6.1 m) has AASHTO specified LLDF equal to 0.10 from both the AASHTO Specifications [4]; [5]. Similar to bridge A, the analytical LLDF envelope has values larger than AASHTO Specifications for all the girders, although the envelope for central girders G9-G14 is close to AASHTO values. The maximum analytical LLDF of exterior girders was observed in G27 which has LLDF of 0.27 and for interior girders was found in G20 which has LLDF of 0.24. Again, the field LLDF envelope has values larger than that for the semi truck for most of the girders. From Table 4, the AASHTO Standard and LRFD provided 34.6% and 16% smaller values relative to the statistical exterior girder limit; 22% and 5.3% smaller values than that for statistical interior girder limit.

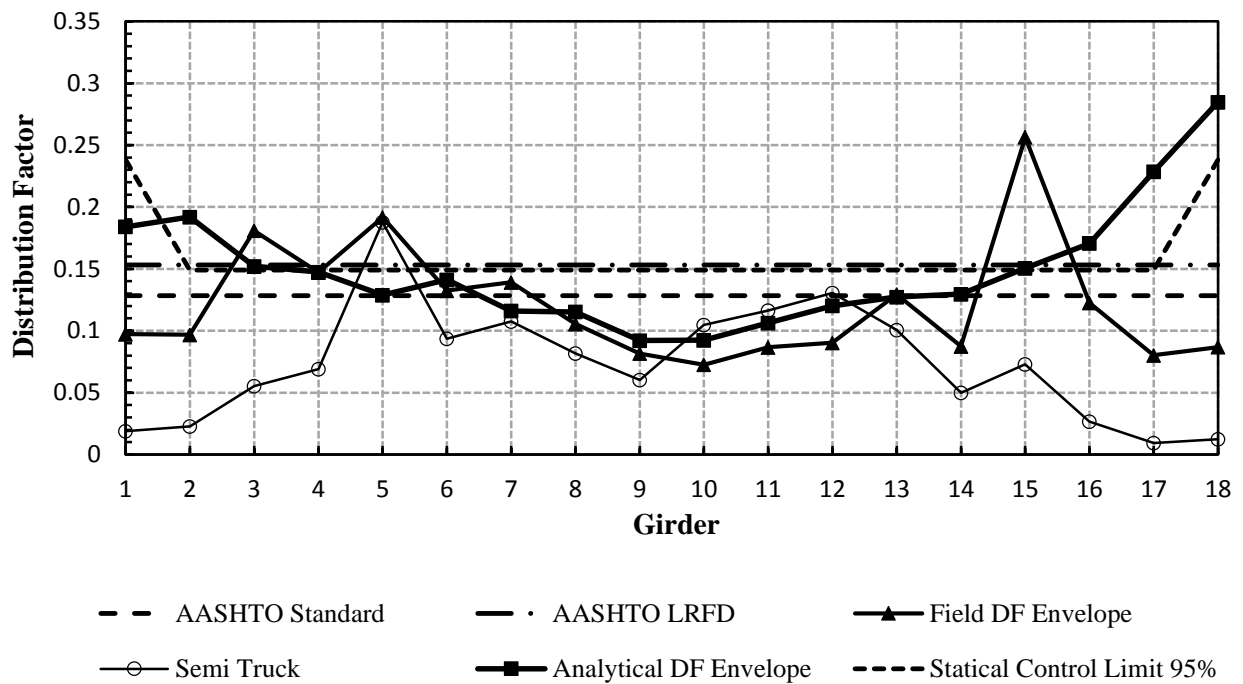


Figure 11: Graphical representation of results for bridge C

The analytical LLDF envelope shown in Figure 12 has greater values than AASHTO Specifications for exterior girders and maximum was observed in girder G18 which has

LLDF of 0.28. For most of the interior girders G5 to G14, the analytical LLDF envelope is lower than AASHTO values. The reason could be uniform girder spacing compared to bridges A and B. Regardless of the lower analytical LLDFs; the concern for a designer will be the maximum value observed in G17 which has LLDF of 0.23. Also, the statistical limits obtained from CDF plots indicate greater values than AASHTO Specifications as shown in Table 4. Similar to bridge A and B, LLDFs of semi five-axle truck are lower than field LLDFs resulting from farm vehicles for almost all the girders.

Based upon the multiple comparisons from Figures 10, 11 and 12, most of the girders for all three bridges have higher analytical LLDFs than the AASHTO Specifications. This tendency may be attributed to the variability in farm vehicles characteristics, the uncertainty in timber components' deterioration, and non-uniform spacing between the girders associated with non-symmetric bridge geometries. It is demonstrated from field testing for all three bridges that the field LLDFs resulting from farm vehicles have mostly higher values as compared to those from typical highway type trucks. This can be due to the difference in vehicle characteristics. Since vastly different characteristics and transverse vehicle positions are considered in the analytical LLDFs' determination, the analytical LLDFs of most girders show high LLDFs for the considered bridges compared to the AASHTO values. Therefore, it can be concluded that the current AASHTO Specification are unsatisfactory for LLDFs determination of timber girder bridges loaded with farm vehicles. Specifically, the AASHTO specified LLDFs are not conservative enough to be considered in designing timber girder bridges under farm loadings. There is a need to develop new equations to consider the effect of farm vehicles on timber girder bridges and include them in the AASHTO Specifications.

Summary and Conclusion

Lateral Live-Load Distribution Factors (LLDFs) for three timber girder bridges loaded with different farm vehicles and a highway vehicle were determined based upon the s-over rule provided by the AASHTO Specifications, field testing, Finite Element Analysis (FEA) model simulations, and statistical analysis. The vehicles used for the field testing

were four heavy farm vehicles and one semi five-axle truck reflecting a conventional highway truck. Field LLDFs were efficient to clearly understand the complicated structural behavior of timber bridges that were selected for this study. Analytical models were created using commercially available FEA based software, and then calibrated with data obtained from field testing. Extensive data on the 121 vehicles having the majority of vehicles frequently used by farmers in the United States were obtained from local farm implement dealers. The complete models of the test bridges were loaded with 121 different farm vehicles covering all the transverse locations. LLDFs calculated from analytical results were used to determine statistical limits of each bridge based upon a fundamental probability theory. All resulting field, analytical, and statistical LLDFs were compared with those resulting from the AASHTO LLDF Specifications based on which the following conclusion were drawn.

1. The analytical LLDFs were greater than AASHTO Specifications in most cases for both exterior and interior girders indicating that AASHTO formulas are not to consider the impact of farm vehicles on the selected bridges.
2. The statistical limits also prove AASHTO Specifications unsatisfactory for all the three timber girder bridges considered.
3. Comparison of field results between farm vehicles and semi five axle truck reveal that farm vehicles result in different LLDFs than conventional highway trucks.
4. AASHTO Specifications consider only girder spacing as major to specify LLDFs. In our study, the selected bridges having non-uniform girder spacing resulted in very high LLDFs. Therefore it is necessary to consider other bridge geometric parameters to determine LLDFs similar to steel-concrete bridges.

It was concluded that the AASHTO formulas were not sufficiently satisfactory for the design and load rating of the selected bridges. This was because of neglecting different characteristics of farm vehicles and its transverse vehicle positions. In the future, hence, the effect of farm vehicular characteristics on LLDFs is needed to develop new AASHTO formulas for timber girder bridges with plank decking. Other geometric parameters of

bridge affecting LLDFs other than girder spacing should be considered as well. Again, there is a need to carry out parametric study to develop reliable LLDF formulas to include all the above effects.

Acknowledgements

This work was sponsored by a pooled fund project administered by the Iowa Department of Transportation. Other sponsors include the Minnesota DOT, Illinois DOT, Nebraska DOT, Oklahoma DOT, Kansas DOT, Wisconsin DOT, and the USDA Forest Products Laboratory.

CHAPTER 3. FARM VEHICLE INDUCED LATERAL LIVE-LOAD DISTRIBUTION FOR STEEL GIRDER BRIDGES WITH PLANK DECKING

Modified from a paper to be submitted to Journal of Engineering Structures

Abstract

The American Association of State Highway and Transportation Officials (AASHTO) Standard and LRFD specifications provide simplified formulae to determine live load distribution factors (LLDFs) for roadway bridges. The AASHTO specified LLDFs are developed considering the effect of typical highway vehicles. As of 2010, the state of Iowa has 24,722 roadway bridges, majority of which consist of bridges on secondary roadways where heavy farm vehicles are frequently allowed. Farm vehicles have a wider range of geometries and weights than conventional highway trucks and thus their variability can result in different LLDFs compared to those of highway trucks. The aim of this paper is hence intended to better predict LLDFs for steel bridges under the effect of farm loadings. The focus is on the determination of LLDFs for steel girder bridges with timber decking through field testing, codified processes, and analytical simulations.

Commercially available finite element analysis (FEA) software was used to generate and refine analytical models of eleven bridges tested with four different farm vehicles and one highway truck with field data. Using over one hundred farm vehicles as live input loads in model simulations, analytical LLDFs were determined from the simulations. Results showed that the analytical and field LLDF values were less than the AASHTO values for one-way traffic bridges and two-way traffic bridges with steel girders spaces narrowly (< 0.81 m). This however conceived unsatisfactory results for two way bridges with wide girder spacing.

Introduction

According to the statistics of National Bridge Inventory (NBI), timber deck bridges constitute approximately ten percent of all bridge types. Surprisingly, Iowa accounts for most number of timber deck bridges amounting to 11% of the total; of which 78% are used on steel beams [1]. The majority consists of bridges on secondary roadways where heavy farm vehicles having wider range of geometries and weights are used for agricultural practices. These characteristics which differ from conventional highway trucks result in dissimilar Live Load Distribution Factors (LLDFs) [16]. LLDFs can generally be defined as the ratio of the maximum live-load effect in a single component to the maximum live-load effect in a system when using beam-line model techniques [3]. The knowledge of LLDFs is needed to determine actual values of live load (truck load) for design of bridge girders. Overestimation of LLDFs can lead to serious economic consequences and underestimation makes the structure deficient to carry required load [22].

American Association of State Highway and Transportation Officials (AASHTO) Specifications (AASHTO Standard 1996; AASHTO LRFD 2010) provide LLDFs for all bridge types. The AASHTO LRFD code [23] specified LLDFs are found out to be more consistent than AASHTO Standard code [4], particularly for bridges with long span lengths [22]. AASHTO codes specify LLDFs for steel girder bridges on timber deck based on a simple *s-over* rule. The *s-over* rule considers only girder spacing to determine LLDFs and ignores the effects of other bridge configuration parameters including span length, bridge width, number of girders, longitudinal stiffness of girders and thickness of the deck. Although, the AASHTO LRFD code [5] was updated with the extensive work of National Cooperative Highway Research Program (NCHRP) report [24], they did not focus their results on steel girder bridges with timber deck and hence the specifications remain the same. In our study, the effect of farm vehicle characteristics on LLDFs was also considered apart from bridge geometric parameters. Therefore, the objective of this study is a validation of code-specified LLDFs for steel girder bridges on timber deck under farm vehicles.

This validation is carried out by field tests and Finite Element Analysis (FEA). Field testing is the most reliable and acceptable means to determine the load carrying capacity of the bridges [25] [26]. This is vindicated by Barker (1999) who states that bridges exhibit higher load carrying capacities than those determined from analytical calculations [27]. In our study, the finite element models were validated with field testing data for reliability and accuracy. Many researchers like Bakht, B. et al. (1987), Zokaie et al. (1988), Kim and Novak (1997) tried to validate load distribution equations for steel-concrete bridges specified by AASHTO Codes using field tests and/or FEA ([10]; [9]; [13]). For example, Bakht B. et al. (1987) examined the basic assumptions upon which AASHTO method of lateral load distribution is based and concluded that some are defensible, others are not [10]. Kim and Novak (1997) performed field tests on steel I-girder bridges and showed that LLDFs were lower than AASHTO Specifications [13]. Taking a step further, Eom and Nowak (2006) performed both field tests and FEA on five two-lane steel girder bridges and showed that AASHTO Code specifications were conservative for LLDF determination [14].

Most of the previous studies on live load distribution were focused on steel girder bridges with concrete deck (steel-concrete). Very few researchers like Hilton and Ichter (1975) investigated load distribution on a steel girder bridge with timber deck (steel-timber) [7]. Their study was focused on a single bridge subject to two conditions which revealed that AASHTO Code specified LLDFs were too high for interior girders and slightly low for exterior girders. Other than Hilton and Ichter, not many investigated load distribution in steel-timber bridges. Also, none of the studies mentioned above considered the effect of farm vehicle characteristics on LLDFs. Meanwhile, a recent study by Seo et al. (2010) shed some light on the effect of agricultural loads on LLDFs for five steel-concrete bridges [16]. The LLDFs which were determined experimentally and analytically revealed values not greater than AASHTO specified values. However, their research was not on steel-timber bridges and hence the need to investigate live load distribution for steel-timber bridges arises. Also, it is necessary to consider the effect of farm vehicles on LLDFs.

This study aims to explore LLDFs of steel-timber bridges under the passage of farm vehicles with different characteristics. The paper is structured into five sections to accomplish the study. The first section presents general information of eleven steel-timber bridges considered for this study. It also includes detailed information for one of the selected eleven bridges which was considered for the procedure. The next section describes various approaches adopted to determine LLDFs for the selected bridges, which include the codified process, field tests, and analytical analysis. Following which, resulting LLDFs obtained from each approach are compared with each other investigating the effect of farm vehicle loadings on load distribution. The final section highlights some insights from this study and provides some recommendations for future work.

Selected Bridges

Eleven continuous single & multi-span steel girder bridges with timber deck (steel-timber) were considered for this research located in Crawford, Boone & Greene counties in Iowa. The bridge characteristics for all the eleven bridges numbered from B1 to B11 are tabulated in Table 5. The table includes National Bridge Inventory (NBI) database identification number and basic geometric information of each bridge. For convenience, the entire approach was presented for one of the eleven bridges selected and then the same was generalized for the remaining.

Table 5: Selected steel-timber bridges' characteristics

Bridge	NBI No.	Number of spans	Span Lengths (m)	Girder Spacing (m)	Number of Girders	Width (m)	Deck thickness (cm)	Skew (deg)
B1	126231	1	9.45, 7.54	0.79	10	7.54	10.16	0
B2	126252	1	10.21, 7.47	0.86	9	7.47	7.62	30
B3	127121	3	10.36, 10.36, 10.36	1.07	7	7.31	10.16	0
B4	120851	2	12.80, 18.28	0.96	8	7.21	10.16	0
B5	128211	1	11.58	0.81	9	6.70	10.16	0
B6	128370	2	7.31, 12.80	0.96	7	6.40	10.16	0
B7	162051	2	6.0, 6.0	0.52	15	7.19	10.16	0
B8	162511	1	8.84	0.53	13	6.22	10.16	7.3
B9	162691	1	9.04	0.52	13	6.19	7.62	0
B10	77470	1	14.07	0.77	8	5.49	7.62	0
B11	77790	3	7.39, 7.39, 7.39	0.34*, 0.94	8	5.49	10.16	0

* – girder spacing between exterior and interior girders

The representative bridge with NBI identification number 120851 is referred as B4 in this study. The bridge B4 is located $42^{\circ}N 2' 56.51''$; $94^{\circ}W 6' 24.80''$, about 20 miles West of Ledges State Park, in Boone County, Iowa. Figure 13 shows the overview of the location of the bridge B4.

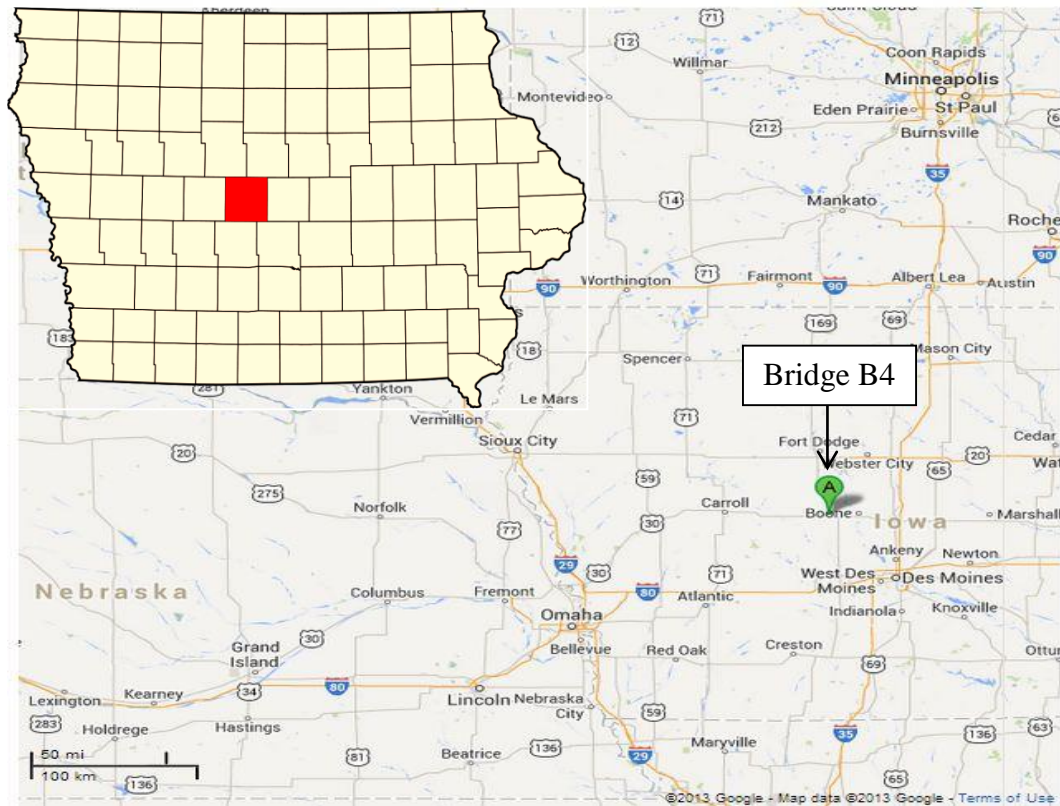


Figure 12: Overview of the location of the bridge B4

Bridge B4 carrying two-way traffic is a continuous two span steel girder bridge with timber deck. The individual lengths of first and second spans are 10.29 m and 12.80 m respectively making up to a total span length of 23.09 m. The width of the bridge is 7.21 m, measured out-to-out of the bridge deck. The photographs of bridge elevation view and condition of steel girders is shown in Figure 14. It has 10.16 cm thick timber deck in satisfactory condition according to Iowa DOT inspection data. The steel girders have I-cross-section of depth 61 cm. Figure 15 shows the cross-section details of longest span of the bridge.



(a)

(b)

Figure 13: Photographs of bridge B4 (a) Elevation view (b) Steel girders

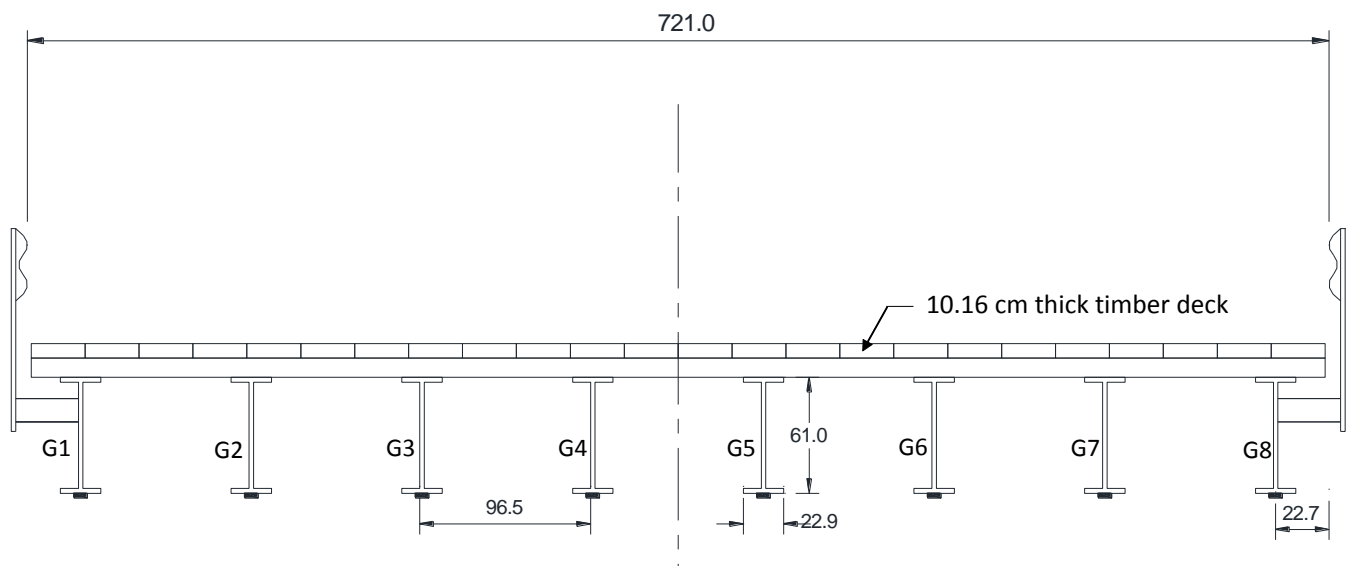


Figure 14: Cross-section of bridge B4

Approaches

LLDFs are determined for the eleven steel girder bridges with timber deck based upon AASHTO Specifications, field testing and FEA simulations whose details are discussed below.

AASHTO Specifications

The AASHTO Specifications provide LLDFs for moment based on s-over rule for steel girder on timber deck bridges [4]; [5]. The simple s-over rule based live load distribution factors for shear and moment have been used for bridge design since the 1930s [24]. These traditional factors are easy to apply, also proved to be overly conservative and sometimes underestimate in some parameter ranges [22]; [24]. The validity and reasonableness of the results from field tests and FEA simulations in our research are evaluated using AASHTO Specifications, based on which suitable recommendations were made.

From Table 3.23.1 in AASHTO Standard Code [4], the Specification of LLDFs for interior steel girders on timber deck is given as

Single lane

$$\frac{S}{14.8} \quad (6)$$

Multiple lanes

$$\frac{S}{13.1} \quad (7)$$

The LLDFs specified by AASHTO Standard Code are for wheel loads [4]. A factor of 0.5 is multiplied for above specifications to be applicable to a full truck [6].

From Tables 4.6.2.2.2a-1 & 4.6.2.2.2b-1 in AASHTO LRFD Code [5], the Specification of LLDFs for interior steel girders on timber deck is given as

Single lane

$$\frac{S}{22.0} \quad (8)$$

Multiple lanes

$$\frac{S}{24.6} \quad (9)$$

Lever rule is recommended by AASHTO Specifications [4]; [5] to determine LLDFs for moment of exterior girders for steel girder bridges with timber deck. The lever rule is a method of computing the LLDFs by summing moments about the first interior girder, assuming a notional hinge to get the reaction at the exterior girder [18]. More details on the *lever rule* can be found in the AASHTO LRFD Specifications [5].

Field Tests

Field testing is a major tool in bridge evaluation. The reasons for testing include uncertainties in material and structural modeling, and concerns for serviceability limit states [28]. Researchers like Peil et al. (2005) tried to predict the life time of old bridges using field data to reduce uncertainties in their analytical models [29]. In our research, field testing was necessary to obtain actual data for determining experimental LLDFs and finite element modeling.

Field testing was carried out using five farm vehicles which include a terragator, a terragator with single front axle, a tractor with a grain wagon, a tractor with one liquid manure applicator tank, and a tractor with two liquid manure applicator tanks. In testing bridges B1 through B6, the normal terragator and tractor with one *half full* liquid manure

applicator tank was used instead of a terragator with one wheel front axle and tractor with two liquid manure applicator tanks. Apart from farm vehicles; a five axle semi-truck was also used in field testing as it is the only conventional highway truck in the inventory, which is used as a benchmark for exploring highway vehicle LLDFs. The photographs and configurations of vehicle inventory are shown in Figure 16 and Table 6 respectively.



(a) Tractor with one liquid manure applicator tank



(b) Tractor with two liquid manure applicator tank



(c) Terragator with single wheel front axle



(d) Terragator with two wheel front axle



(e) Tractor grain wagon



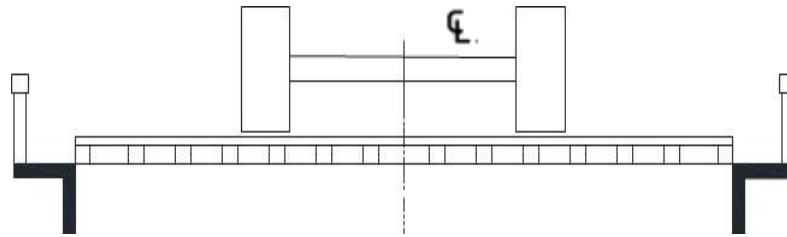
(f) Five axle semi-truck

Figure 15: Photographs of vehicles used for field testing

Table 6: Vehicle configurations used for field testing

Vehicle	Weight (KN)					Length of the vehicle (m)	
	Front Axle	Rear Axle	Grain Wagon	Tank	Trailer		
Tractor with one tank	48.7	70.0	-	118.8	-	237.5	12.3
Tractor with two tanks	47.1	101.4	-	180.7	-	329.2	12.3
Terragator	104.0	73.3	-	-	-	177.3	5.8
Terragator with single front axle	49.2	144.2	-	-	-	193.4	7.8
Tractor Grain Wagon	108.9	87.6	53.3	-	-	249.8	9.5
Semi-Truck	47.9	150.6	-	-	147.2	345.7	15.9

During the testing process, one test vehicle was driven at a time across the bridge at a crawl speed of approximately 5-10 kmph. The vehicles were driven along the centerline of the bridge as shown in Figure 17.

**Figure 16:** Location of vehicle during field testing

A network of multiple strain gages was attached to bottom flanges of all steel girders to record the strain as the vehicle passes the bridge. The entire data acquisition system was acquired from Bridge Diagnostics Inc. (BDI) [19]. Figure 18 shows the sample plot of strain data of all the test vehicles for one of the steel girders of bridge B4. It was observed that all the girders are subjected to more strain when farm vehicles were passed compared to the semi-truck. Figure 19 shows the strain plot of all the girders when the semi-truck passes the bridge B4. As the vehicles were made through the center of the bridge, max strain was observed in the central girders (G3, G4 and G5) of the bridge compared to exterior girders (G1 and G8). The strain data acquired was employed to calculate experimental LLDFs for each girder using the following equation [30].

$$DF^f = \frac{\mathcal{E}^m_{\max i, t}}{\sum_{i=1}^n \mathcal{E}^m_{\max i, t}} \quad \text{or} \quad \frac{M^m_{\max i, t}}{\sum_{i=1}^n M^m_{\max i, t}} \quad (10)$$

Where DF^f is the field distribution factor; \mathcal{E}^m and M^m are the measured maximum strains and moments for individual girders over time, respectively.

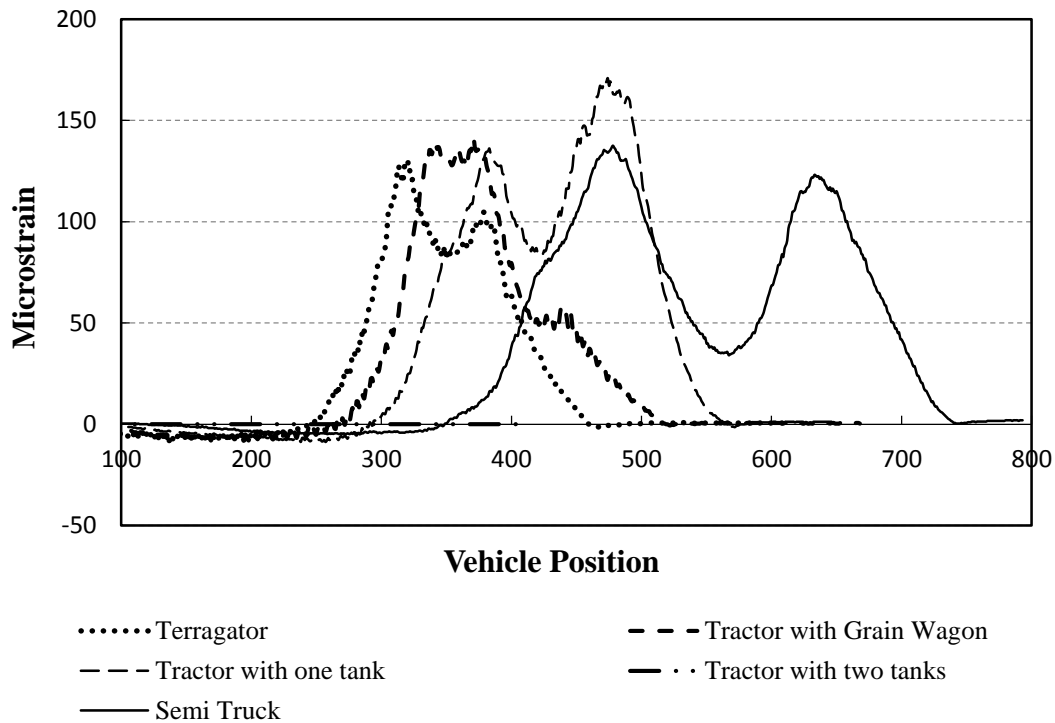


Figure 17: Sample strain plot of all test vehicles

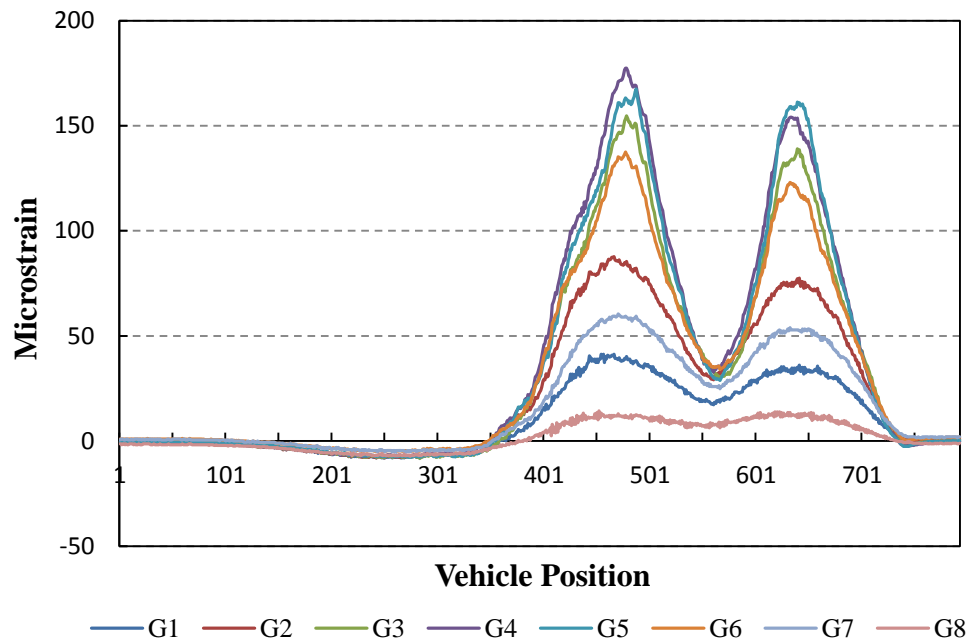


Figure 18: Strain plot of all girders for bridge B4

FEA Simulations

Field testing requires great effort and an expensive procedure to adopt every time to evaluate LLDFs. In our study, we considered a vehicle inventory of 121 farm vehicles and it is not practically possible to field test every bridge with every farm vehicle of interest. Therefore, finite element modeling is considered to be an accurate and efficient method for the analytical analysis of bridges, especially when we are considering large number of vehicular loads. Many researchers like Fanous et al., Bishara et al. and Elisa et al. used finite element models to determine analytical LLDFs [6]; [12]; [31]. A detailed description of the procedure adopted is presented in the following subsections.

Model Generation and Calibration

The model generation was done by implementing the technique proposed by Seo et al. [16]. A finite element model is developed for each of the eleven bridges using the software acquired from Bridge Diagnostics Inc. [19]. The user interface of the software

requires geometric information of the bridge, which was obtained from the bridge plans and/or field inspections as shown in Table 5. The finite element model considers steel girders as beam elements and timber deck as shell elements. The modulus of elasticity for each shell element of the timber was used as 11031.6 MPa, taken from AASHTO LRFD Code [5]. Rotational springs are defined to simulate the actual behavior of supports at abutments and bearings at piers; boundary conditions are defined accordingly. Figure 20 shows the finite element model of representative bridge B4 loaded with terragator.

After modeling the bridge, the finite element model was calibrated with field data. The model calibration is defined as an iterative process to obtain the highest correlation and the lowest error between the analytical and measured field responses. The aim was to make the model the most accurate so that it predicts the actual behavior of the bridge in the field. This was accomplished by calibrating physical and material properties of the bridge elements within reasonable limits that were based on previous research work by Seo et al. 2013 [16]. The calibration parameters considered were similar for all the eleven bridges; which include moment of inertia of steel girders along the axes perpendicular to the cross-section, modulus of elasticity of timber deck and rotational stiffness at the supports. For each step in the iteration process, the values of the parameters are modified within the reasonable limits set up. A graphical user interface tool available in the software was used to make comparisons between field and analytical results. Initial and calibrated values of the parameters are summarized in Table 7 for the eleven bridges. The model accuracy is measured by a parameter “percent error (δ_p)” which measures the variation of analytical result from field testing data and tells how well the model is able to predict the real behavior of the bridge in-situ.

For the representative bridge B4, single cross-sections were used for all the calibration parameters including steel girders, deck elements and supports at the end. The model was calibrated with an accuracy was 93.2% and percent error of 6.8% predicting the actual behavior of the bridge to the maximum extent. Similar to bridge B4, all the remaining ten bridge models were calibrated to an accuracy of more than 90%. Unlike for bridge B4, different cross-sections were considered for exterior and interior girders in the case of

bridges B7, B8 and B9 as cross-section of exterior girders was different from that of interior girders.

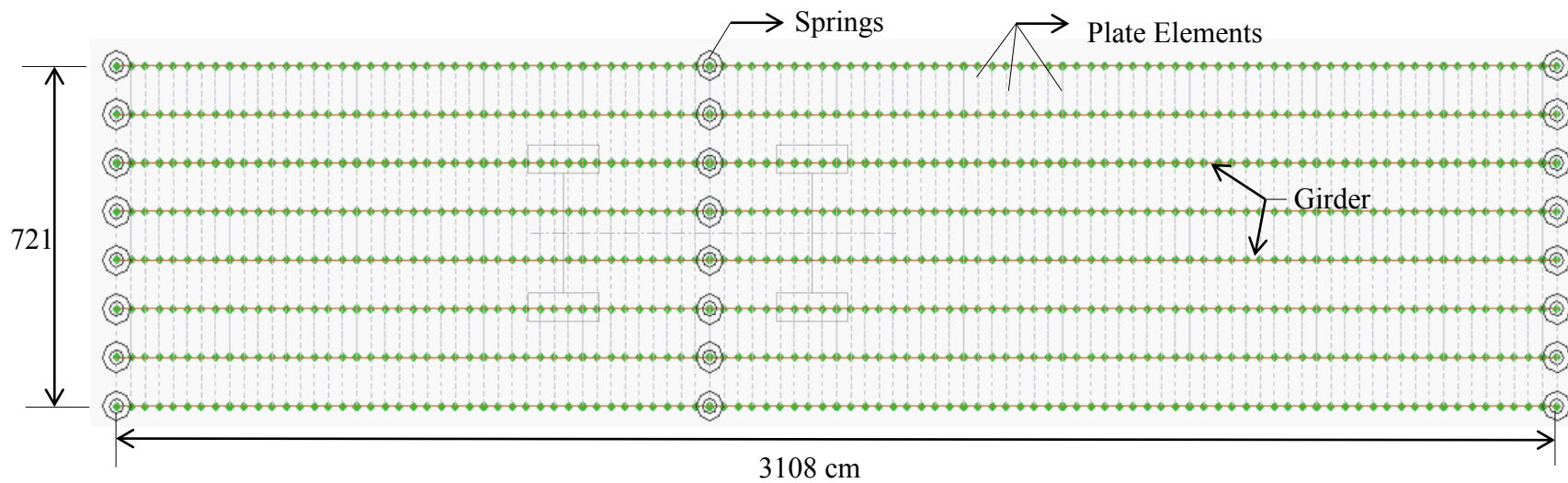


Figure 19: Finite element model of bridge B4 loaded with terragator

Table 7: Initial and calibrated values for bridge structural components

Bridge		Calibration Parameters			
		Moment of Inertia (cm ⁴)		Young's Modulus (Mpa)	Rotational Stiffness (kN-cm/rad)
		Exterior Girder	Interior Girder	Deck	Support Connections (Springs)
B1	Original	1.57E+04	1.57E+04	1.10E+04	0.00E+00
	Calibrated	1.56E+04	1.56E+04	1.07E+04	9.33E+05
B2	Original	5.18E+04	5.18E+04	1.10E+04	0.00E+00
	Calibrated	4.85E+04	4.85E+04	1.34E+04	2.60E+06
B3	Original	8.66E+04	8.66E+04	1.10E+04	0.00E+00
	Calibrated	6.73E+04	6.73E+04	8.62E+03	6.99E+06
B4	Original	9.80E+04	9.80E+04	1.10E+04	0.00E+00
	Calibrated	9.80E+04	9.80E+04	1.03E+04	1.76E+06
B5	Original	2.04E+04	2.04E+04	1.10E+04	0.00E+00
	Calibrated	2.04E+04	2.04E+04	8.27E+03	1.13E+05
B6	Original	1.35E+05	1.35E+05	1.10E+04	0.00E+00
	Calibrated	1.04E+05	1.04E+05	1.10E+04	8.88E+05
B7	Original	1.07E+04	1.42E+04	1.10E+04	0.00E+00
	Calibrated	1.07E+04	1.42E+04	8.27E+03	2.42E+05
B8	Original	1.09E+04	1.42E+04	1.10E+04	0.00E+00
	Calibrated	1.09E+04	1.42E+04	9.40E+03	3.91E+05
B9	Original	8.99E+03	1.53E+04	1.10E+04	0.00E+00
	Calibrated	1.09E+04	1.91E+04	8.27E+03	4.35E+03
B10	Original	6.75E+04	6.75E+04	1.10E+04	0.00E+00
	Calibrated	6.94E+04	6.94E+04	1.36E+04	6.74E+05
B11	Original	1.75E+04	1.75E+04	1.10E+04	0.00E+00
	Calibrated	1.32E+04	1.32E+04	1.38E+04	9.75E+05

Vehicle Implementation

To investigate the variability of vehicle configuration on DFs, information of 121 farm vehicles was collected from farm equipment manufacturers and suppliers nationwide. These 121 farm vehicles have different axle spacing, weights, and gage widths. Detailed characteristics for the farm vehicles are included in Appendix and can also be found elsewhere in the previous study by Seo et al. 2013 [16]. Each calibrated model was applied by each of 121 farm vehicles through an automation process developed specially for this study. The vehicles are made to cross each model covering all the transverse locations. The transverse location determines the vehicle position in the lateral direction. Note that number of transverse locations for each vehicle depends upon its axle width and bridge width measured from curb to curb. Figure 20 shows a sample transverse location of the vehicle terragator on bridge B4. The strain gages were defined for each model at the same locations as the field testing was done. The strain values recorded for each vehicle are used to determine analytical LLDFs using the Eq. (10).

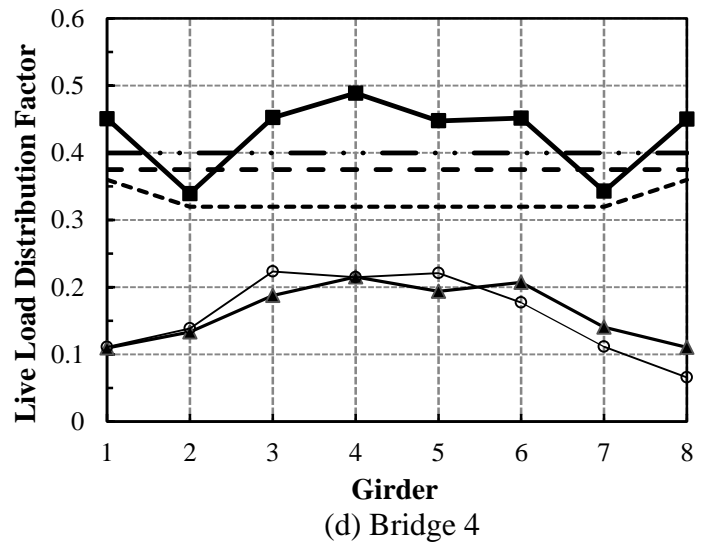
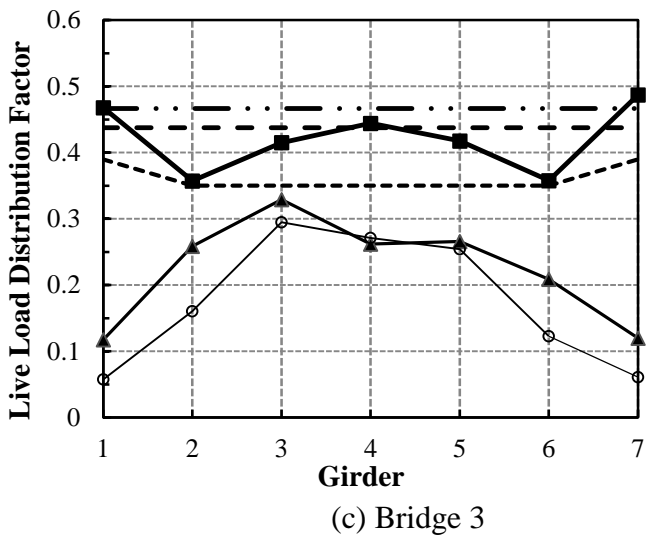
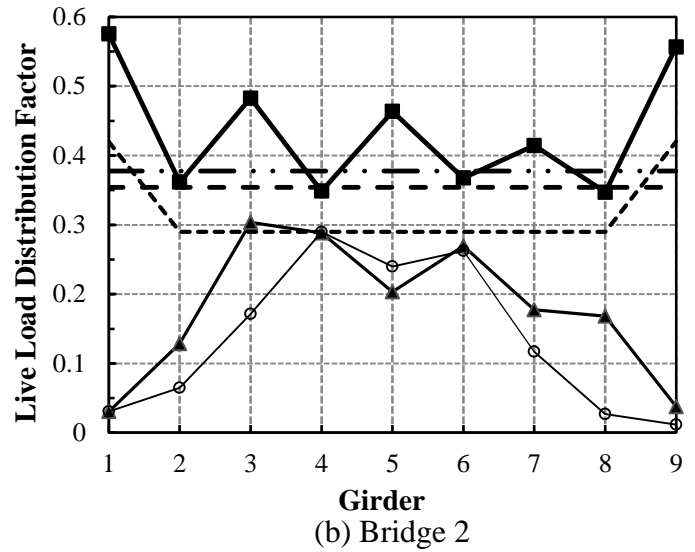
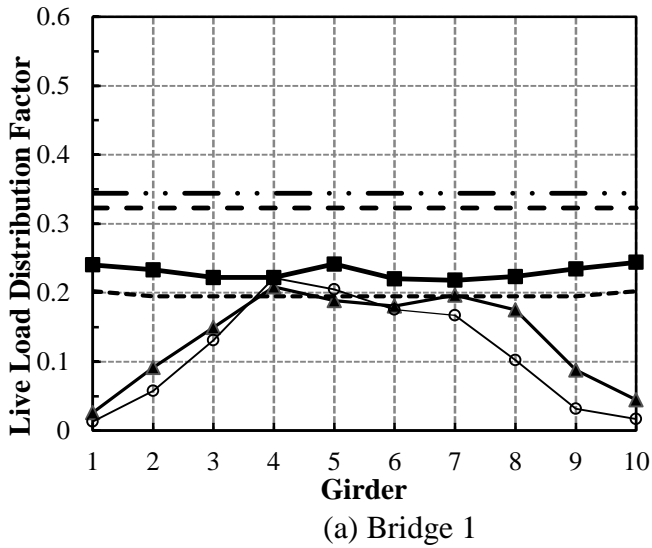
Results and Discussion

Figure 20(a-k) show the LLDFs for the eleven Steel-Timber bridges. Figure 20(a) for Bridge 1 shows that the Analytical LLDFs for all exterior girders and interior girders are smaller than those from the AASHTO Specifications. The bridge showed a consistent behavior for all the steel girders. Similarly, the Field LLDF envelope and semi truck LLDFs for the interior and exterior girders are less than the AASHTO Standard and LRFD values. The statistical limit for interior girders was 40% and 43% smaller than the AASHTO Standard and LRFD values, respectively and the exterior girder limit was 47% and 50% smaller, respectively. For Bridge 1, Analytical LLDF and Field LLDF envelopes are, in most cases, larger than semi truck plot.

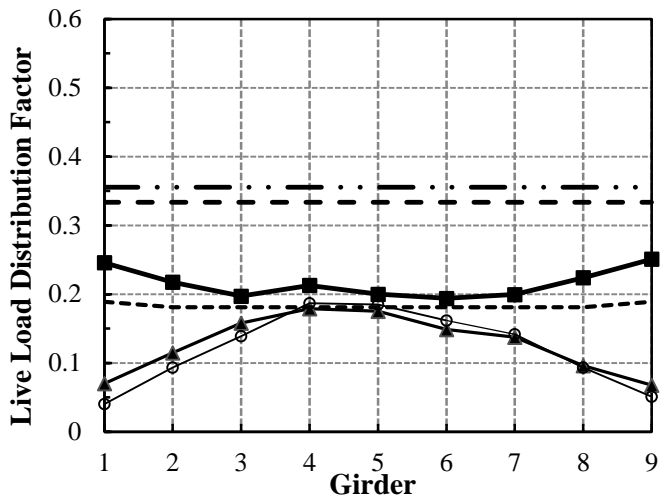
The Analytical LLDFs for all the girders of all the eleven Steel-Timber bridges are summarized in Table 8 along with both AASHTO ones. As AASHTO Codes specify single LLDF values for exterior and interior girders, the statistical limits for exterior and interior girders are also included. The Analytical LLDFs higher than AASHTO values are bold. For almost all the bridges, the AASHTO Specifications proved to be conservative. The Analytical LLDFs exceeded AASHTO values for Bridges 2, 3, 4 and 6 in case of exterior girders and Bridges 2 and

4 in case of interior girders. The statistical limits were lower than AASHTO values for all the bridges except for exterior girders for Bridge 2. The variability of LLDFs in Bridge 2 can be attributed to skewness of the bridge. When a farm vehicle of axle width of 10 ft. is made to run across Bridge 2 of 24.5 ft wide and 30 degrees skew angle; there is chance that one wheel is on the bridge and other is completely off the bridge; causing unexpected moment on the girders which result in indifferent LLDFs.

The Field LLDFs were greater than LLDFs from semi truck in most girders for all the bridges. Also, the Field LLDFs for farm vehicles and a five axle semi truck were, in most cases, less than both the AASHTO Standard and LRFD values for all the eleven bridges.



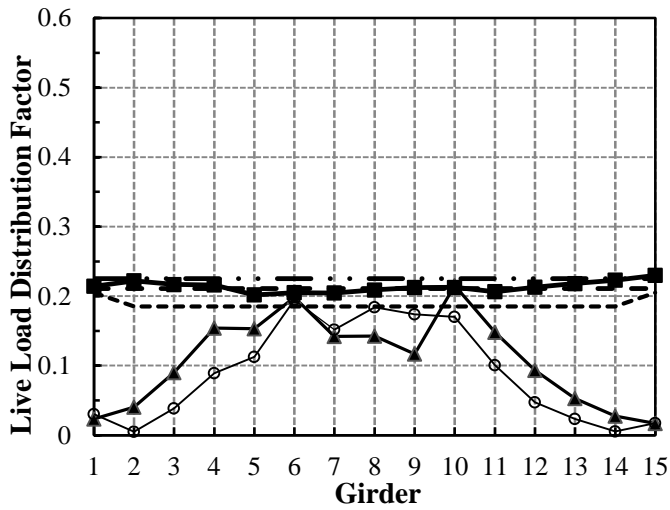
AASHTO Standard
 AASHTO LRFD
 ▲ Field LLDF Envelope
○ Semi Truck
 ■ Analytical LLDF Envelope
 Statistical Limit 95%



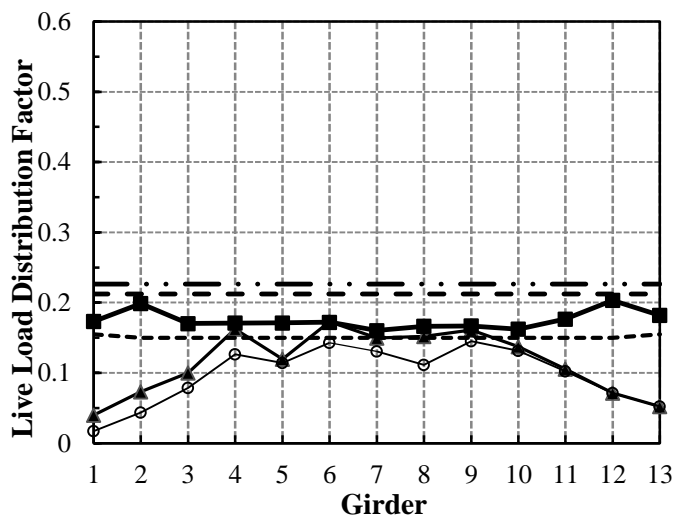
(e) Bridge 5



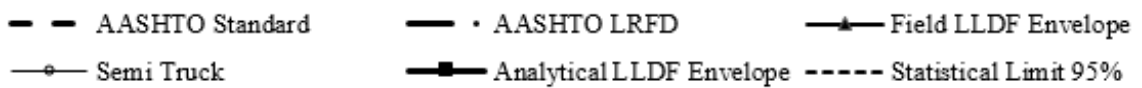
(f) Bridge 6

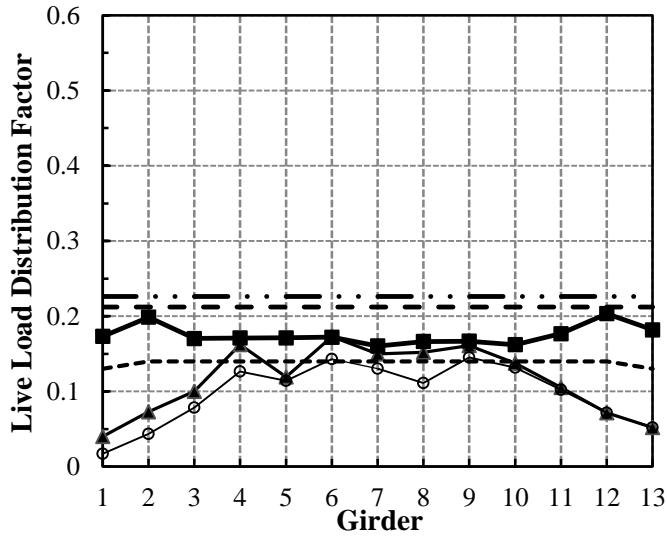


(g) Bridge 7

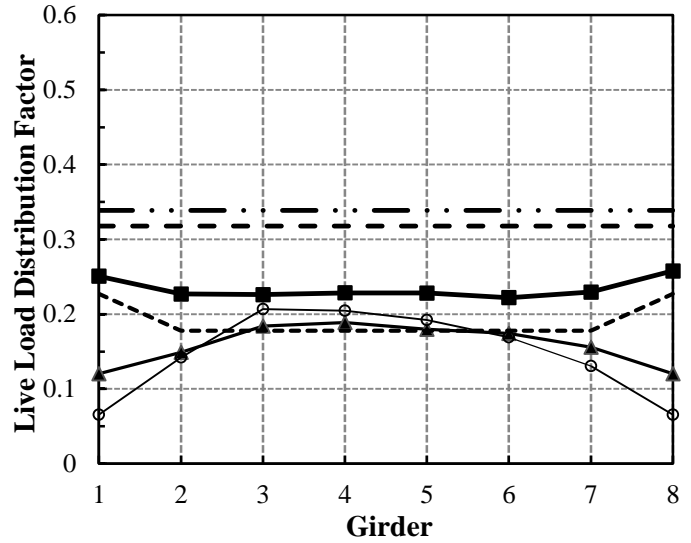


(h) Bridge 8





(i) Bridge 9



(j) Bridge 10



(k) Bridge 11

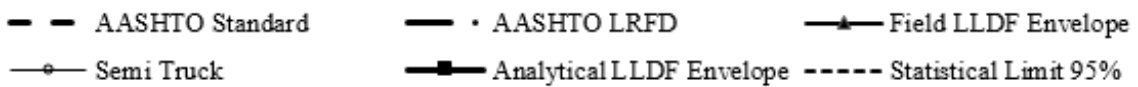


Figure 20:(a-k) LLDFs for Field Tested Steel-Timber bridges

Table 8: Comparison of Analytical and AASHTO Specified LLDFs for Field Tested Steel-Timber Bridges

Bridge	Analytical LLDFs for Girders															Statistical Limit		AASHTO Codes	
	G1	G2	G3	G4	G5	G6	G7	G8	G9	G10	G11	G12	G13	G14	G15	Interior Girders	Exterior Girders	LRFD	Standard
1	0.24	0.23	0.22	0.22	0.24	0.22	0.22	0.22	0.23	0.24						0.19	0.20	0.34	0.32
2	0.58	0.36	0.48	0.35	0.46	0.37	0.41	0.35	0.56							0.29	0.42	0.38	0.35
3	0.47	0.36	0.41	0.44	0.42	0.36	0.49									0.35	0.39	0.47	0.44
4	0.45	0.34	0.45	0.49	0.45	0.45	0.34	0.45								0.32	0.36	0.42	0.40
5	0.25	0.22	0.20	0.21	0.20	0.19	0.20	0.22	0.25							0.18	0.19	0.36	0.33
6	0.52	0.37	0.38	0.39	0.35	0.38	0.52									0.31	0.37	0.42	0.40
7	0.21	0.22	0.22	0.22	0.20	0.21	0.20	0.21	0.21	0.21	0.21	0.21	0.22	0.22	0.23	0.19	0.21	0.23	0.21
8	0.17	0.20	0.17	0.17	0.17	0.17	0.16	0.17	0.17	0.16	0.18	0.20	0.18			0.15	0.16	0.23	0.21
9	0.16	0.20	0.17	0.17	0.17	0.17	0.16	0.17	0.17	0.17	0.17	0.20	0.16			0.14	0.12	0.23	0.21
10	0.25	0.23	0.23	0.23	0.23	0.22	0.23	0.26								0.19	0.23	0.38	0.28
11	0.32	0.32	0.33	0.35	0.35	0.33	0.32	0.32								0.20	0.29	0.34	0.41

Note: The highlighted values in the table indicated that analytical LLDFs greater than AASHTO Specified LLDFs in that particular case

The percent differences AASHTO values and statistical limits was calculated for all bridges and summarized in Table 9. For Bridge 5, the AASHTO Standard and LRFD LLDFs were the most conservative compared to Analytical LLDFs among all the eleven bridges; greater than exterior girder statistical limit by 43% and 47% respectively, and 46% and 49% greater than interior girder statistical limit respectively. Bridges 4 and 6 have the same girder spacing and AASHTO Codes provide same LLDFs. It was observed that Bridges 4 and 6 have different Analytical LLDFs indicating that other bridge characteristics are important in determining LLDFs. Bridge 2 has exterior girder statistical limits greater than AASHTO values by 19% and 11% respectively.

Table 9: Percent difference between AASHTO Specified LLDFs and Statistical Limits for Field Tested Steel-Timber Bridges

Bridge	Exterior Girder Statistical Limit		Interior Girder Statistical Limit	
	AASHTO Standard	AASHTO LRFD	AASHTO Standard	AASHTO LRFD
1	37%	41%	40%	44%
2	-19%	-11%	18%	23%
3	11%	16%	20%	25%
4	9%	15%	19%	24%
5	43%	47%	46%	49%
6	7%	12%	22%	27%
7	0%	7%	10%	16%
8	24%	29%	29%	33%
9	44%	47%	34%	39%
10	19%	39%	33%	50%
11	30%	15%	52%	42%

Note: The negative sign in indicates that Analytical LLDF is higher than AASHTO LLDF

Summary and Conclusion

This study involved the evaluation of the effect of farm implements of husbandry on load distribution equations of existing steel girder bridges with timber deck (steel-timber)

specified in AASHTO Design Specifications. This was accomplished by carrying out field testing on eleven in-service steel-timber bridges. The data obtained from field testing consists of strain values recorded under the passage of five test vehicles including four farm vehicles and a five axle semi-truck. This field data was used to validate / calibrate analytical Finite Element Analysis (FEA) models developed utilizing commercially available software for each of the eleven bridges. The validated FEA models were used to perform analytical study using an inventory of 121 farm vehicles with a broad range of varying vehicular characteristics. The 121 farm vehicles were made to run across each of the FEA models covering different transverse locations. A large number of analytical Distribution Factors (LLDFs) were computed for each girder from the model simulations of all the bridges. The maximum LLDF for each girder was identified and the envelope of analytical LLDF for each bridge was then compared with those of field tests, AASHTO Standard and LRFD Codes. The objective was to verify whether current AASHTO equations could include the effect of farm vehicle loadings from which the following conclusions were drawn.

1. The interior and exterior Analytical LLDFs for farm vehicles were smaller than the AASHTO design values (Standard and LRFD) in most cases for all the eleven bridges. Bridges with identical girder spacing have different Analytical LLDFs for both exterior and interior girders, which is not covered by AASHTO Specifications based on s-over rule.
2. Comparisons between the statistical limits and AASHTO design values revealed that AASHTO codes for all the eleven bridges are conservative for steel interior and exterior girders.
3. The measured Field LLDFs for farm vehicles and a five axle semi truck were, in most cases, smaller than AASHTO design values for all the eleven bridges.

The analytical results include the effect of all the parameters of bridge geometry and vehicle characteristics on the girder LLDFs. The study recommends including the effect of vehicular characteristics on LLDFs by incorporating vehicular characteristics in AASHTO specified equations. It also acknowledges developing better sophisticated

equations by including other bridge geometric parameters to determine live load distribution, similar to steel girder bridges with concrete deck. As the vehicle characteristics used in this research were similar to the farm vehicles used in real world, the behavior of the timber girder bridges to these loads are known and hence these results can be incorporated into the future design of bridges. It also helps in selecting girder LLDFs for bridges of similar kind and serve as a basis for developing niche equations for live load distribution for steel girder bridges with timber deck.

Acknowledgements

This work was sponsored by a pooled fund project administered by the Iowa Department of Transportation. Other sponsors include the Minnesota DOT, Illinois DOT, Nebraska DOT, Oklahoma DOT, Kansas DOT, Wisconsin DOT, and the USDA Forest Products Laboratory.

REFERENCES

- [1] P. C. Pierce, "Heavy Timber Decks on Steel Beam Bridges," *ASCE Structures Congress*, p. 13, 2010.

- [2] M. A. Ritter, "Timber Bridges: Design, Construction, Inspection and Maintenance," US Department of Agriculture, Washington, D.C., 1990.

- [3] Barker and Puckett, *Design of Highway Bridges: Based on AASHTO LRFD specifications*, New York: John Wiley and Sons, 2007.

- [4] AASHTO, *Standard specifications for highway bridges*, Washington, D.C., 1996.

- [5] AASHTO, *LRFD bridge design specifications*, Washington, D.C., 2010.

- [6] J. M. T. W. Fouad Fanous, "Development of Live-Load Distribution Factors for Glued Laminated Timber Girder Bridges," *ASCE Journal of Bridge Engineering*, vol. 16, no. 2, p. 9, 2010.

- [7] M. H. Hilton and L. L. Ichter, "An Investigation of the Load Distribution on a Timber Deck-Steel Girder Bridge," Virginia Highway & Transportation Research Council, Charlottesville, Virginia, 1975.

- [8] P. J. Barr, M. O. Eberhard and J. F. Stanton, "Live Load Distribution Factors in Prestressed Concrete Girder Bridges," *ASCE Journal of Bridge Engineering*, vol. 6, no. 5, p. 9, 2001.

- [9] T. Zokaie, R. A. Imbsen and T. A. Osterkamp, "Distribution of Wheel Loads on Highway Bridges," in *Transportation Research Board*, 1992.
- [10] F. M. Bakht. B, "Lateral Distribution Factors for Highway Bridges," *ASCE Journal of Structural Engineering*, vol. VIII, p. 19, 1987.
- [11] K. Tarhini and a. Frederick, "Wheel Load Distribution in I-Girder Highway Bridges," *ASCE Journal of Structural Engineering*, vol. 118, no. 5, p. 10, 1992.
- [12] A. L. M. E.-A. N. Bishara, "Wheel Load Distribution on Simply Supported Skew I-Beam Composite Bridges," *ASCE Journal of Structural Engineering*, vol. 119, no. 2, p. 21, 1993.
- [13] N. A. S. Kim. S, "Load Distribution and Impact Factors for I-Girder Bridges," *ASCE Journal of Bridge Engineering*, p. 8, 1997.
- [14] J. Eom and A. S. Nowak, "Validation of Code Specified Girder Distribution for Continuous Steel Girder Bridges," *ASCE Structures Congress*, p. 11, 2006.
- [15] D. Elisa, Sotelino and a. J. Liu, "Simplified Load Distribution Factors for use in LRFD Design," Joint Transportation Research Program, West Lafayette, Indiana, 2004.
- [16] J. Seo, B. Phares and T. Wipf, "Lateral Live-Load Distribution Characteristics of Simply Supported Steel Girder Bridges Loaded with Implements of Husbandry," *Journal of Bridge Engineering*, 2013.

- [17] M. A. a. D. S. R. Ritter, "Research Accomplishments for Wood Transportation Structures based on National Research Needs Assessment," Forest Service, Forest Products Laboratory, Madison, WI, 1998.
- [18] S. BridgeSight, "Live Load Distribution Factors for a Three Span Continuous Precast Girder Bridge," BridgeSight Software, Rescue, California, 1999.
- [19] BDI, "Bridge Diagnostics Inc.," Bridge Dianostics Inc., 2010. [Online]. Available: <http://bridgetest.com/>.
- [20] L. B. Roger, "Distribution Factors for Curved I-Girder Bridges," *ASCE Journal of Structural Engineering*, vol. 112, no. 10, p. 16, 1986.
- [21] K. Phuvoravan, "Load Distribution Factor Equation for Steel Girder Bridges in LRF Design," University of Philippines, Quezon, 2006.
- [22] A. S. N. Junsik Eom, "Live Load Distribution for Steel Girder Bridges," *Journal Of Bridge Engineering*, vol. 6, p. 9, 2001.
- [23] AASHTO, LRF bridge design specifications, Washington, D.C., 1998.
- [24] T. Transportation Research Board, "National Cooperative Highway Research Program (NCHRP) Report 592," Washington, D.C., 2007.
- [25] S. F. B. S. A. C. Andrew Jeffrey, "Evaluation of Bridge Performance and Rating through Non-destructive Load Testing," Vermont Agency of Transportation, Vermont, Virginia, 2009.

- [26] L. G. J. Baider Bakht, "Bridge Testing - A Surprise Every Time," *Journal of Structural Engineering*, vol. 116, no. 5, p. 14, 1990.
- [27] M. G. Barker, "Steel Girder Bridge Field Test Procedures," *Construction and Building Materials*, vol. 13, no. 4, p. 11, 1999.
- [28] J. P. L. R. B. Fred Moses, "Applications of Field Testing To Bridge Evaluation," *Journal of Structural Engineering*, p. 18, 1992.
- [29] U. M. M. Peil, M. Frenz and R. Scharff, "Life Time Prediction of Old Bridges," *Material Science and Engineering Technology*, vol. 36, no. 11, p. 7, 2005.
- [30] T. Hosteng, "Live Load Deflection Criteria for Glued Laminated Structures," Iowa State University, Ames, IA, 2004.
- [31] J. a. A. S. N. A. Elisa, "Validation of Code-Specified Girder Distribution for Continuous Steel Girder Bridges," *ASCE Journal of Structural Engineering*, p. 11, 2006.
- [32] Newmark, "Design of I-Beam Bridges," *ASCE Journal of Structural Engineering*, 1948.
- [33] D. Huang, T. Wang and a. S. M., "Impact Studies of Multigirder Concrete Bridges," *ASCE Journal of Structural Engineering*, vol. 119, no. 8, p. 15, 1993.

APPENDIX – FARM VEHICLE INVENTORY

Farm Vehicle Inventory includes 121 farm vehicles and implements that were used in the study. Through internet searches and manufacturer inquiries, information regarding axle weights and configurations was gathered for 121 farm vehicles and implements. These combinations encompassed most combinations seen on US secondary roadway bridges.

The table below summarizes the characteristics of the Farm Vehicle Inventory. The table classifies each vehicle as grain cart or tanker or agricultural truck depending on the use. It also includes the number of axles, axle spacing and weight of each axle and spacing between consecutive axles. This information was used to model the vehicular input loads on the finite element models.

No	NAME	CLASS	AXLES	Axle spacing (ft)						Axle Weight (lbs)						Spacing between consecutive axles (ft)				
				1	2	3	4	5	6	1	2	3	4	5	6	1	2	3	4	5
1	Grain Semi	Semi Trailer	4	6.1	6.1	6.1	6.1			17300	17460	16600	16720			4.0	4.0	4.0		
2	John Deere 8520 & Kinze 1050 ROW	Grain Cart	3	7.0	7.0	7.0				11525	11525	73381			9.9	23.9				
3	John Deere 8520 & Houle 3-axle Tank	Manure Tanker	5	7.0	7.0	7.0	7.0	7.0		11525	11525	26600	26600	26600	9.9	14.8	5.7	5.7		
4	John Deere 8520 & Houle 2-axle Tank	Manure Tanker	4	7.0	7.0	7.0	7.0			11525	11525	31290	31290		9.9	17.5	5.7			
5	New Holland TD5050 & Houle 3-axle Tank	Manure Tanker	5	6.6	6.6	7.0	7.0	7.0		8070	8070	26600	26600	26600	7.7	15.0	5.7	5.7		
6	New Holland TD5050 & Houle 2-axle Tank	Manure Tanker	4	6.6	6.6	7.0	7.0			8070	8070	31290	31290		7.7	18.0	5.7			
7	New Holland TD5050 & Kinze 1050 ROW	Grain Cart	3	6.6	6.6	7.0				8070	8070	73381			7.7	24.6				
8	New Holland T4040 & Houle 3-axle Tank		5	5.1	5.1	7.0	7.0	7.0		6724	6724	26600	26600	26600	7.2	15.0	5.7	5.7		
9	New Holland T4040 & Houle 2-axle Tank		4	5.1	5.1	7.0	7.0			6724	6724	31290	31290		7.2	18.0	5.7			
10	New Holland T4040 & Kinze 1050 Row		3	5.1	5.1	7.0				6724	6724	73381			7.2	24.6				
11	John Deere 8520 & Balzer 6350 Narrow	Manure Tanker	4	7.0	7.0	7.3	7.3			11525	11525	36183	36183		9.9	24.3	5.6			
12	New Holland TD5050 & Balzer 6350 Narrow	Manure Tanker	4	6.6	6.6	7.3	7.3			8070	8070	36183	36183		7.7	24.5	5.6			
13	New Holland T4040 & Balzer 6350 Narrow		4	5.1	5.1	7.3	7.3			6724	6724	36183	36183		7.2	24.5	5.6			
14	Terragator 8400	Agricultural Truck	2	7.0	7.5					9338	10758				16.8					
15	John Deere 8520 with Brent 1082 Grain Wagon		3	7.0	7.0	7.8				11525	11525	15660			9.9	23.9				
16	New Holland TD5050 with Grain Wagon	Agricultural Truck	3	6.6	6.6	7.8				8070	8070	15660			7.7	23.9				
17	New Holland T4040 with Grain Wagon		3	5.1	5.1	7.8				6724	6724	15660			7.2	23.9				
18	John Deere 8520 & Better-Bilt 3400	Manure Tanker	4	7.0	7.0	7.9	7.9			11525	11525	18421	18421		9.9	22.7	4.1			
19	New Holland TD5050 & Better-Bilt 3400	Manure Tanker	4	6.6	6.6	7.9	7.9			8070	8070	18421	18421		7.7	23.0	4.1			
20	New Holland T4040 & Better-Bilt 3400		4	5.1	5.1	7.9	7.9			6724	6724	18421	18421		7.2	23.0	4.1			
21	Terragator 7300	Agricultural Truck	2	0.0	8.0					9338	10758				22.8					
22	John Deere 8520 & Kinze 1050 SOF	Grain Cart	3	7.0	7.0	8.0				11525	11525	72101			9.9	23.9				
23	John Deere 8520 & Better-Bilt 4950	Manure Tanker	4	7.0	7.0	8.0	8.0			11525	11525	27252	27252		9.9	25.3	4.4			
24	New Holland TD5050 & Better-Bilt 4950	Manure Tanker	4	6.6	6.6	8.0	8.0			8070	8070	27252	27252		7.7	25.5	4.4			
25	New Holland TD5050 & Kinze 1050 SOF	Grain Cart	3	6.6	6.6	8.0				8070	8070	72101			7.7	24.6				
26	New Holland T4040 & Better-Bilt 4950		4	5.1	5.1	8.0	8.0			6724	6724	27252	27252		7.2	25.5	4.4			
27	New Holland T4040 & Kinze 1050 SOF		3	5.1	5.1	8.0				6724	6724	72101			7.2	24.6				
28	Terragator 2505	Agricultural Truck	3	0.0	8.0	8.0				11060	16200	16200			19.2	6.4				
29	Versatile 280 & Kinze 1050 ROW	Grain Cart	3	8.0	8.0	7.0				11800	15900	73381			10.7	24.0				
30	Versatile 280 & Kinze 1050 SOF	Grain Cart	3	8.0	8.0	8.0				11800	15900	72101			10.7	24.0				
31	Versatile 280 & Better-Bilt 4950	Manure Tanker	4	8.0	8.0	8.0	8.0			11800	15900	27252	27252		10.7	25.5	4.4			
32	Versatile 280 & Better-Bilt 3400	Manure Tanker	4	8.0	8.0	7.9	7.9			11800	15900	18421	18421		10.7	23.0	4.1			
33	Versatile 280 & Balzer 6350 Narrow	Manure Tanker	4	8.0	8.0	7.3	7.3			11800	15900	36183	36183		10.7	24.5	5.6			
34	Versatile 280 & Houle 3-axle Tank	Manure Tanker	5	8.0	8.0	7.0	7.0	7.0		11800	15900	26600	26600	26600	10.7	15.0	5.7	5.7		
35	Versatile 280 & Houle 2-axle Tank	Manure Tanker	4	8.0	8.0	7.0	7.0			11800	15900	31290	31290		10.7	18.0	5.7			
36	Versatile 280 with Half Full Houle 7300 Tank	Agricultural Truck	5	8.0	8.3	8.0	8.0	8.0		11800	15900	16267	16267	16267	10.7	18.4	5.8	5.8		

37	John Deere 8520 & Better-Bilt 6600	Mamure Tanker	5	7.0	7.0	8.4	8.4	8.4	11525	11525	24826	24826	24826	9.9	23.6	5.2	5.2	
38	Versatile 280 & Better-Bilt 6600	Mamure Tanker	5	8.0	8.0	8.4	8.4	8.4	11800	15900	24826	24826	24826	10.7	24.0	5.2	5.2	
39	New Holland TD5050 & Better-Bilt 6600	Mamure Tanker	5	6.6	6.6	8.4	8.4	8.4	8070	8070	24826	24826	24826	7.7	24.0	5.2	5.2	
40	New Holland T4040 & Better-Bilt 6600		5	5.1	5.1	8.4	8.4	8.4	6724	6724	24826	24826	24826	7.2	24.0	5.2	5.2	
41	Case 340B		3	8.5	8.5	8.5			31614	16160	16160			13.7	6.8			
42	John Deere 9200 & Kinze 1050 ROW	Grain Cart	3	8.7	8.7	7.0			18840	18660	73381			11.3	24.0			
43	John Deere 9200 & Kinze 1050 SOF	Grain Cart	3	8.7	8.7	8.0			18840	18660	72101			11.3	24.0			
44	John Deere 9200 & Better-Bilt 6600	Mamure Tanker	5	8.7	8.7	8.4	8.4	8.4	18840	18660	24826	24826	24826	11.3	24.0	5.2	5.2	
45	John Deere 9200 & Better-Bilt 4950	Mamure Tanker	4	8.7	8.7	8.0	8.0		18840	18660	27252	27252		11.3	25.5	4.4		
46	John Deere 9200 & Better-Bilt 3400	Mamure Tanker	4	8.7	8.7	7.9	7.9		18840	18660	18421	18421		11.3	23.0	4.1		
47	John Deere 9200 & Balzer 6350 Narrow	Mamure Tanker	4	8.7	8.7	7.3	7.3		18840	18660	36183	36183		11.3	24.5	5.6		
48	John Deere 9200 & Houle 3-axle Tank	Mamure Tanker	5	8.7	8.7	7.0	7.0	7.0	18840	18660	26600	26600	26600	11.3	15.0	5.7	5.7	
49	John Deere 9200 & Houle 2-axle Tank	Mamure Tanker	4	8.7	8.7	7.0	7.0		18840	18660	31290	31290		11.3	18.0	5.7		
50	John Deere 9200 with Brent 1082 Grain Wagon	Agricultural Truck	3	8.7	8.7	7.8			18840	18660	15660			11.3	23.9			
51	Case 380 & Better-Bilt 6600	Mamure Tanker	5	8.7	8.7	8.4	8.4	8.4	20240	16060	24826	24826	24826	12.9	24.0	5.2	5.2	
52	Case 380 & Better-Bilt 4950	Mamure Tanker	4	8.7	8.7	8.0	8.0		20240	16060	27252	27252		12.9	25.5	4.4		
53	Case 380 & Better-Bilt 3400	Mamure Tanker	4	8.7	8.7	7.9	7.9		20240	16060	18421	18421		12.9	23.0	4.1		
54	Case 380 & Balzer 6350 Narrow	Mamure Tanker	4	8.7	8.7	7.3	7.3		20240	16060	36183	36183		12.9	24.5	5.6		
55	Case 380 & Houle 3-axle Tank	Mamure Tanker	5	8.7	8.7	7.0	7.0	7.0	20240	16060	26600	26600	26600	12.9	15.0	5.7	5.7	
56	Case 380 & Houle 2-axle Tank	Mamure Tanker	4	8.7	8.7	7.0	7.0		20240	16060	31290	31290		12.9	18.0	5.7		
57	Case 380 & Kinze 1050 ROW	Grain Cart	3	8.7	8.7	7.0			20240	16060	73381			12.9	24.6			
58	Case 380 & Kinze 1050 SOF	Grain Cart	3	8.7	8.7	8.0			20240	16060	72101			12.9	24.6			
59	Case 380 with Brent 1082 Grain Wagon		3	8.7	8.7	7.8			20240	20240	15660			12.9	23.9			
60	John Deere 8520 with 2 Empty NUHN QT Quad Tanks	Agricultural Truck	6	7.0	7.0	9.5	9.5	9.5	11525	11525	7150	7150	9150	9.9	21.0	6.3	17.2	6.3
61	John Deere 9200 with 2 Empty NUHN QT Quad Tanks	Agricultural Truck	6	8.7	8.7	9.5	9.5	9.5	18840	18660	7150	7150	9150	11.3	21.0	6.3	17.2	6.3
62	New Holland TD5050 with 2 Empty NUHN QT Quad Tanks		6	6.6	6.6	9.5	9.5	9.5	8070	8070	7150	7150	9150	7.7	18.0	6.3	17.2	6.3
63	New Holland T4040 with 2 Empty NUHN QT Quad Tanks		6	5.1	5.1	9.5	9.5	9.5	6724	6724	7150	7150	9150	7.2	18.0	6.3	17.2	6.3
64	Case 380 with 2 Empty NUHN QT Quad Tanks	Agricultural Truck	5	8.7	8.7	9.5	9.5	9.5	20240	16060	7150	7150	9150	12.9	21.0	6.3	17.2	6.3
65	John Deere 9620 & Kinze 1050 ROW	Grain Cart	3	9.7	9.7	7.0			20175	20175	73381			11.5	24.6			
66	John Deere 9620 & Kinze 1050 SOF	Grain Cart	3	9.7	9.7	8.0			20175	20175	72101			11.5	24.6			
67	John Deere 9620 & Better-Bilt 6600	Mamure Tanker	5	9.7	9.7	8.4	8.4	8.4	20175	20175	24826	24826	24826	11.5	24.3	5.2	5.2	
68	John Deere 9620 & Better-Bilt 4950	Mamure Tanker	4	9.7	9.7	8.0	8.0		20175	20175	27252	27252		11.5	26.0	4.4		
69	John Deere 9620 & Better-Bilt 3400	Mamure Tanker	4	9.7	9.7	7.9	7.9		20175	20175	18421	18421		11.5	23.4	4.1		
70	John Deere 9620 & Balzer 6350 Narro	Mamure Tanker	4	9.7	9.7	7.3	7.3		20175	20175	36183	36183		11.5	25.0	5.6		
71	John Deere 9620 & Houle 3-axle Tank	Mamure Tanker	5	9.7	9.7	7.0	7.0	7.0	20175	20175	26600	26600	26600	11.5	15.5	5.7	5.7	
72	John Deere 9620 & Houle 2-axle Tank	Mamure Tanker	4	9.7	9.7	7.0	7.0		20175	20175	31290	31290		11.5	18.2	5.7		
73	John Deere 9620 with Brent 1082 Grain Wagon	Agricultural Truck	3	9.7	9.7	7.8			20175	20175	15660			11.5	23.9			
74	John Deere 9620 with 2 Empty NUHN QT Quad Tanks	Agricultural Truck	6	9.7	9.7	9.5	9.5	9.5	20175	20175	7150	7150	9150	11.5	21.0	6.3	17.2	6.3
75	John Deere 9620 & Balzer 1250	Grain Cart	4	9.7	9.7	10.0	10.0		20175	20175	43512	43512		11.5	21.9	6.5		
76	John Deere 9620 & Balzer 1500	Grain Cart	5	9.7	9.7	10.0	10.0	10.0	20175	20175	34443	34443	34443	11.5	18.6	6.5	6.5	
77	John Deere 8520 & Balzer 1250	Grain Cart	4	7.0	7.0	10.0	10.0		11525	11525	43512	43512		9.9	21.2	6.5		
78	John Deere 8520 & Balzer 1500	Grain Cart	5	7.0	7.0	10.0	10.0	10.0	11525	11525	34443	34443	34443	9.9	17.9	6.5	6.5	
79	John Deere 9200 & Balzer 1250	Grain Cart	4	8.7	8.7	10.0	10.0		18840	18660	43512	43512		11.3	21.5	6.5		
80	John Deere 9200 & Balzer 1500	Grain Cart	5	8.7	8.7	10.0	10.0	10.0	18840	18660	34443	34443	34443	11.3	18.0	6.5	6.5	

81	Versatile 280 & Balzer 1250	Grain Cart	4	8.0	8.0	10.0	10.0											11800	15900	43512	43512							10.7	21.5	6.5				
82	Versatile 280 & Balzer 1500	Grain Cart	5	8.0	8.0	10.0	10.0	10.0										11800	15900	34443	34443	34443						10.7	18.0	6.5	6.5			
83	Case 380 & Balzer 1250	Grain Cart	4	8.7	8.7	10.0	10.0										20240	16060	43512	43512							12.9	21.9	6.5					
84	Case 380 & Balzer 1500	Grain Cart	5	8.7	8.7	10.0	10.0	10.0								20240	16060	34443	34443	34443							12.9	18.6	6.5	6.5				
85	New Holland TD5050 & Balzer 1250	Grain Cart	4	6.6	6.6	10.0	10.0									8070	8070	43512	43512									7.7	21.9	6.5				
86	New Holland TD5050 & Balzer 1500	Grain Cart	5	6.6	6.6	10.0	10.0	10.0								8070	8070	34443	34443	34443									7.7	18.6	6.5	6.5		
87	New Holland T4040 & Balzer 1250		4	5.1	5.1	10.0	10.0									6724	6724	43512	43512									7.2	21.9	6.5				
88	New Holland T4040 & Balzer 1500		5	5.1	5.1	10.0	10.0	10.0								6724	6724	34443	34443	34443									7.2	18.6	6.5	6.5		
89	Case 600 with 2 Empty NUHN QT Quad Tanks		6	10.0	10.0	9.5	9.5	9.5	9.5							23000	23000	7150	7150	9150	9150									12.8	18.0	6.3	17.2	6.3
90	Case 600 with Grain Wagon		3	10.0	10.0	7.8										23000	23000	15660												12.8	23.9			
91	Case 600 & Better-Bilt 6600		5	10.0	10.0	8.4	8.4	8.4								23000	23000	24826	24826	24826									12.8	24.0	5.2	5.2		
92	Case 600 & Better-Bilt 4950		4	10.0	10.0	8.0	8.0									23000	23000	27252	27252										12.8	25.5	4.4			
93	Case 600 & Better-Bilt 3400		4	10.0	10.0	7.9	7.9									23000	23000	18421	18421										12.8	23.0	4.1			
94	Case 600 & Balzer 6350 Narrow		4	10.0	10.0	7.3	7.3									23000	23000	36183	36183										12.8	24.5	5.6			
95	Case 600 & Houle 3-axle Tank		5	10.0	10.0	7.0	7.0	7.0								23000	23000	26600	26600	26600									12.8	15.0	5.7	5.7		
96	Case 600 & Houle 2-axle Tank		4	10.0	10.0	7.0	7.0									23000	23000	31290	31290										12.8	18.0	5.7			
97	Case 600 & Kinze 1050 Row		3	10.0	10.0	7.0										23000	23000	73381											12.8	24.6				
98	Case 600 & Kinze 1050 SOF		3	10.0	10.0	8.0										23000	23000	72101											12.8	24.6				
99	Case 600 & Balzer 1250		4	10.0	10.0	10.0	10.0									23000	23000	43512	43512										12.8	21.9	6.5			
100	Case 600 & Balzer 1500		5	10.0	10.0	10.0	10.0	10.0								23000	23000	34443	34443	34443										12.8	18.6	6.5	6.5	
101	Versatile 535 with 2 Empty NUHN QT Quad Tanks		6	10.0	10.0	9.5	9.5	9.5	9.5							22500	22500	7150	7150	9150	9150									12.8	18.0	6.3	17.2	6.3
102	Versatile 535 with Grain Wagon		3	10.0	10.0	7.8										22500	22500	15660												12.8	23.9			
103	Versatile 535 & Better-Bilt 6600		5	10.0	10.0	8.4	8.4	8.4								22500	22500	24826	24826	24826										12.8	24.0	5.2	5.2	
104	Versatile 535 & Better-Bilt 4950		4	10.0	10.0	8.0	8.0									22500	22500	27252	27252											12.8	25.5	4.4		
105	Versatile 535 & Better-Bilt 3400		4	10.0	10.0	7.9	7.9									22500	22500	18421	18421											12.8	23.0	4.1		
106	Versatile 535 & Balzer 6350 Narrow		4	10.0	10.0	7.3	7.3									22500	22500	36183	36183											12.8	24.5	5.6		
107	Versatile 535 & Houle 3-axle Tank		5	10.0	10.0	7.0	7.0	7.0								22500	22500	26600	26600	26600										12.8	15.0	5.7	5.7	
108	Versatile 535 & Houle 2-axle Tank		4	10.0	10.0	7.0	7.0									22500	22500	31290	31290											12.8	18.0	5.7		
109	Versatile 535 & Kinze 1050 Row		3	10.0	10.0	7.0										22500	22500	73381												12.8	24.6			
110	Versatile 535 & Kinze 1050 SOF		3	10.0	10.0	8.0										22500	22500	72101												12.8	24.6			
111	Versatile 535 & Balzer 1250		4	10.0	10.0	10.0	10.0									22500	22500	43512	43512											12.8	21.9	6.5		
112	Versatile 535 & Balzer 1500		5	10.0	10.0	10.0	10.0	10.0								22500	22500	34443	34443	34443											12.8	18.6	6.5	6.5
113	John Deere 9620 & J&M 1075-22	Grain Cart	3	9.7	9.7	12.2										20175	20175	68700												11.5	19.5			
114	John Deere 8520 & J&M 1075-22	Grain Cart	3	7.0	7.0	12.2										11525	11525	68700												9.9	18.8			
115	John Deere 9200 & J&M 1075-22	Grain Cart	3	8.7	8.7	12.2										18840	18660	68700												11.3	19.0			
116	Versatile 280 & J&M 1075-22	Grain Cart	3	8.0	8.0	12.2										11800	15900	68700												10.7	19.0			
117	Case 380 & J&M 1075-22	Grain Cart	3	8.7	8.7	12.2										20240	16060	68700												12.9	19.5			
118	New Holland TD5050 & J&M 1075-22	Grain Cart	3	6.6	6.6	12.2										8070	8070	68700												7.7	19.5			
119	New Holland T4040 & J&M 1075-22		3	5.1	5.1	12.2										6724	6724	68700												7.2	19.5			
120	Case 600 & J&M 1075-22		3	10.0	10.0	12.2										23000	23000	68700												12.8	19.5			
121	Versatile 535 & J&M 1075-22		3	10.0	10.0	12.2										22500	22500	68700												12.8	19.5			